Dalton Transactions

Extraction and coordination studies of carbonyl−phosphine oxide scorpionate ligand with uranyl and lanthanide(III) nitrates: structural, spectroscopic and DFT characterization of complexes in solid state and solutions

Journal:	*Dalton Transactions*
Manuscript ID	DT-ART-12-2015-004963.R1
Article Type:	Paper
Date Submitted by the Author:	28-Jan-2016

Complete List of Authors:	Matveeva, Anna; Nesmeyanov Institute of Organoelement Compounds, Russian Academy of Sciences, Laboratory of Organophosphorus compounds Vologzhanina, Anna; Nesmeyanov Institute of organoelement compounds, Russian Academy of Sciences, Goryunov, Evgenii; Nesmeyanov Institute of Organoelement Compounds, Russian Academy of Sciences, Laboratory of Organophosphorus compounds Aysin, Rinat; A.N.Nesmeyanov Institute of Organoelement Compounds RAS, Pasechnik, Margarita; Nesmeyanov Institute of Organoelement Compounds, Russian Academy of Sciences, Laboratory of Organophosphorus compounds Matveev, Sergey; Nesmeyanov Institute of Organoelement Compounds, Russian Academy of Sciences , Laboratory of Organophosphorus compounds Godovikov, Ivan; A.N. Nesmeyanov Institute of Organoelement Compounds Russian Academy of Sciences (INEOS RAS), ; Safiulina, Alfiya; OJSC United Chemical Company Uralchem Brel, Valery; A. N. Nesmeyanov Institute of Organoelement Compounds, Russian Academy of Sciences, Laboratory of phosphorus organic compounds

Extraction and coordination studies of carbonyl−phosphine oxide scorpionate ligand with uranyl and lanthanide(III) nitrates: structural, spectroscopic and DFT characterization of complexes in solid state and solutions†

Anna G. Matveeva,[a] Anna V. Vologzhanina,[a] Evgenii I. Goryunov,[a] Rinat R. Aysin,[a] Margarita P. Pasechnik,[a] Sergey V. Matveev,[a] Ivan A. Godovikov,[a] Alfiya M. Safiulina,[b] Valery K. Brel[a]*

[a]*Nesmeyanov Institute of Organoelement Compounds, Russian Academy of Sciences, 28 Vavilov Str., Moscow 119991, Russia*
[b] *OJSC United Chemical Company Uralchem, Presnenskaya nab. 6/2, Moscow, 123317 Russia*

*Corresponding author. Email: matveeva@ineos.ac.ru;
Tel.: +7-4991359366 Fax: +7-4991355085

† Electronic supplementary information (ESI) available: Selected IR data for complexes **1**, **3**–**6**, X-ray data for compounds **L**, **1**–**5**, selected NMR spectra for compounds **L**, **1, 3**, **6**, and extraction data for **L** and **L'**. CCDC 1442097-1442102. For ESI and crystallographic data in CIF or other electronic format see DOI: …….

Abstract

Hybrid scorpionate ligand $(OPPh_2)_2CHCH_2C(O)Me$ (**L**) was synthesized and characterized by spectroscopic methods and X-ray diffraction. The selected coordination chemistry of **L** with $UO_2(NO_3)_2$ and $Ln(NO_3)_3$ (Ln = La, Nd, Lu) has been evaluated. The isolated mono- and binuclear complexes, namely, $[UO_2(NO_3)_2\mathbf{L}]$ (**1**), $[\{UO_2(NO_3)\mathbf{L}\}_2(\mu_2\text{-}O_2)]\cdot EtOH$ (**2**), $[La(NO_3)_3\mathbf{L}_2]\cdot 2.33MeCN$ (**3**), $[Nd(NO_3)_3\mathbf{L}_2]\cdot 3MeCN$ (**4**), $[Nd(NO_2)_2\mathbf{L}_2]^+\cdot(NO_3)^-\cdot EtOH$ (**5**) and $[Lu(NO_3)_3\mathbf{L}_2]$ (**6**) have been characterized by IR spectroscopy and elemental analysis. The single crystal X-ray structures have been determined for complexes **1**–**5**. Intramolecular intraligand π-stacking interaction between two phenyl fragments of the coordinated ligand(s) is observed in all complexes **1**–**5**. π-Stacking interaction energy was estimated from Bader's AIM theory calculations performed on DFT level. Solution properties have been examined by IR and multinuclear (^1H, ^{13}C, and ^{31}P) NMR spectroscopy in CD_3CN and $CDCl_3$. Coordination modes of **L** vary with the coordination polyhedron of the metal and solvent nature showing many coordination modes: P(O),P(O), P(O),P(O),C(O), P(O),C(O), and P(O). Preliminary extraction studies of U(VI) and Ln(III) (Ln = La, Nd, Ho, Yb) from 3.75 M HNO_3 into $CHCl_3$ show that scorpionate **L** extracts *f*-block elements (especially uranium) better than its unmodified prototype $(OPPh_2)_2CH_2$.

1. Introduction

Bidentate neutral organophosphorus extractants, first of all phosphine oxides (carbamoylphosphine oxides, alkylenediphosphine dioxides), are the most efficient extractants for recovery of transplutonium, rare earth, and other elements from wastes of spent nuclear fuel reprocessing to recover different metals from processing solutions of hydrometallurgy and to design analytical test objects for the same metals.[1-4] These compounds are also important in medicine for diagnosis and treatment of different pathologies, mainly locomotor apparatus. The design of novel functionalized phosphine oxides showing higher efficiency and selectivity is one of the major and topical fields of extractive and synthetic chemistry.

Thus, highly efficient extractants for recovery of actinides and rare earth elements from nitric acid solutions were found among derivatives of methylenediphosphine dioxide[2-5] [Scheme 1, (a)–(b)], this fact favored the development of coordination chemistry of these ligands, in particular their ability to coordinate ions of *f*-block elements[6-8].

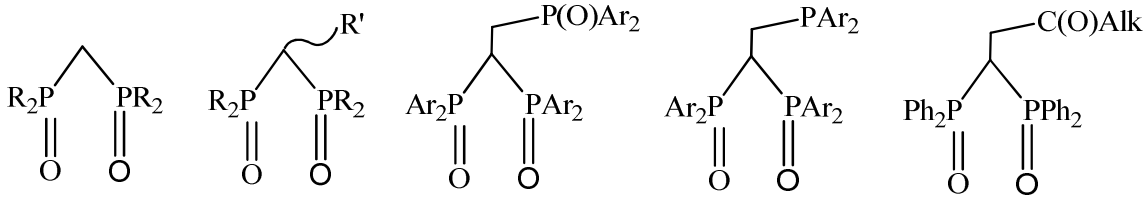

(a) (b) (c) (d) (e)

R = Ar, Alk, AlkO R' = Alk, Ar, CH_2X

Scheme 1. Structures of different types of ligands bearing >P(O)CH_2P(O)<

The introduction of $Ar_2P(O)CH_2$ and Ar_2PCH_2 functional groups showing coordination ability into the methylene bridge of dioxide [Scheme 1, (a)] leads to new scorpionate ligands [Scheme 1, (c)–(d),)] that are promising extractants for nuclear fuel reprocessing.[9] All strongly donating $Ar_2P(O)$ and Ar_2P groups of these scorpionates as expected participate in coordination to lanthanide-like Y(III).[9] The coordination properties of such a scorpionate ligand change considerably if donor phosphorus-containing group in substituent $Ar_2P(O)CH_2$–, Ar_2PCH_2– is replaced by less basic AlkC(O)– group [Scheme 1, (e)]. Less basic carbonyl group may not form coordination bonds with cation or form weaker bonds than phosphorus functionalities as well as participate in other *weak* interactions. Consequently, such a modification can change considerably not only coordination but also extractive properties of the ligand.

In this paper, we report the modified synthesis of a scorpionate ligand $[Ph_2P(O)]_2CHCH_2C(O)Me$ (**L**) and its new complexes with uranyl and lanthanide(III) nitrates, the structural characterization of all compounds in solid state (X-ray for **L**, **1**–**5**) and in solution by IR and multinuclear NMR (^1H, ^{13}C, ^{31}P) spectroscopy, and extraction studies toward f-block elements Furthermore, we report herein the results of AIM analysis (Bader's "Atoms in molecules" approach) for π-stacking interaction in U(VI), La(III), and Nd(III) complexes. Extraction ability of ligand **L** for recovery of U(VI) and Ln(III) from nitric acid solution into chloroform in comparison to $Ph_2P(O)CH_2P(O)Ph_2$ (**L'**) prototype was evaluated.

2. Results and discussion

2.1. Synthesis and characterization of the ligand L.

We prepared compound **L** *via* a modified variant[10] of the Conant reaction[11] that consists in the combining Ph_2PCl with (*E*)-4-(dipenylphosphoryl)but-3-en-2-one, we developed the synthesis of the latter earlier[12]. The reaction was conducted in anhydrous acetonitrile solution at ambient temperature with addition of acetic acid (Scheme 2). Under these conditions, the reaction completed over 48 h to give 4,4-bis(dipenylphosphoryl)butan-2-one (**L**) in 90% yield (according to $^{31}P\{^1H\}$ NMR spectra of reaction mixture). It should be noted that this is the first example of the successful use of the Conant reaction for the synthesis of *gem*-diphosphoryl-substituted alkanones.

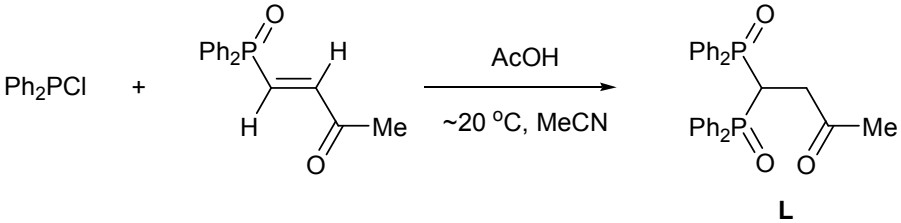

L

Scheme 2. Synthesis of 4,4-bis(diphenylposphoryl)butan-2-one (**L**)

The ligand **L** has been characterized by elemental analysis, IR, ^{1}H, $^{31}P\{^{1}H\}$, and ^{13}C NMR spectroscopy. Thus, in particular, the ^{1}H NMR spectrum of this compound, whose molecule contains two identical diphenylphosphoryl groups, shows the proton signals of CH_2 and CH groups as doublet of triplets and triplet of triplets, respectively, which transform into doublet and triplet under broad band ^{1}H-^{31}P decoupling ($^{1}H\{^{31}P\}$ NMR spectrum). $^{13}C\{^{1}H\}$ NMR spectrum also shows triplets of C=O and CH carbon atoms due to spin-spin coupling with phosphorus nuclei of two $Ph_2P(O)$ groups. IR spectrum of a crystalline sample of **L** exhibits ν(P=O) bands at 1202 and 1182 cm^{-1} and ν(C=O) band at 1720 cm^{-1}. The data of the DFT computation for normal vibrations frequencies of ligand **L** agree well with experimental values without any scaling.[13]

In addition to spectral experiment, compound **L** was characterized in the solid state using single-crystal X-ray diffraction study. Scorpionate ligand **L** displays typical bond lengths and angles, with oxygen atoms of phosphoryl groups trans-situated in respect to the C13 atom (Fig. 1). Selected bond distaces are given in Table 1. Such conformation of **L** is additionally stabilized with π-stacking between the phenyl groups of different phosphorus functionalities (the centroid-centroid distance is equal to 3.681(2) Å and the dihedral angle between the ring planes is equal to 10.81(8)°). Thus, the realization of a bi- and tridentate coordination mode for this ligand requires rotation of donor arms as compared with its conformation in the solid. All three donor groups are involved into weak intra- and intermolecular C–H….O interactions. Intermolecular C_{Ph}-H…O contacts are the most significant. The shortest r(H...O) distances are 2.60 Å for carbonyl group, 2.28, 2.38 Å (for P1–O1) and 2.46, 2.62 Å (for P2–O2) for phosphoryl groups (Fig. S1, ESI†).

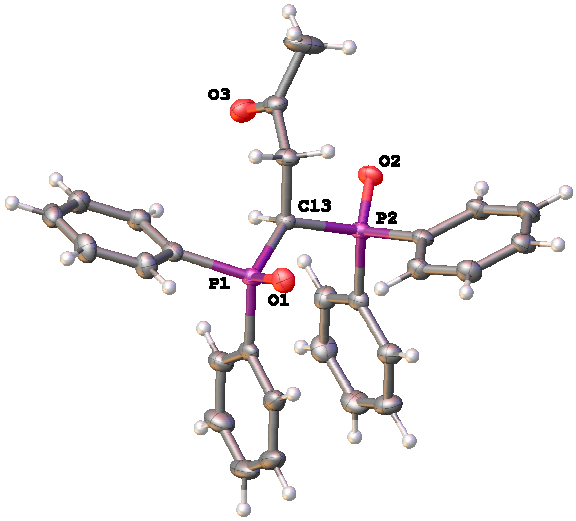

Fig 1. General view of the **L** given in representation of atoms in thermal ellipsoids drawn at p = 50 %.

As far as we know, compound **L** is the first example of hybrid scorpionate ligand combining two P(O) and one C(O) side arms that has been ever characterized in solid state.

Table 1. Selected bond distances (Å) in **L**, and uranyl complexes **1** and **2**

Bond	**L**	**1**	**2**
P1=O1	1.485(1)	1.500(2)	1.487(6)
P2=O2	1.493(1)	1.503(2)	1.495(6)
C=O	1.208(2)	1.213(4)	1.202(12)
U1=O1		1.761(2)	1.877(11)
U1=O2		1.760(2)	1.658(12)
U1 – O3(L)/O9(L)		2.393(2)	2.397(6)
U1 – O4(L)/O8(L)		2.398(2)	2.463(6)
U1 – O(nitrate)		2.506(3) – 2.540(3)	2.520(7) – 2.549(7)
U1 – O(peroxo)			2.361(12) – 2.407(12)

2.2. Synthesis and solid state characterizations of complexes

Compound **L** is a hybrid scorpionate ligand with a combination of two phosphoryl and one carbonyl groups. Therefore the coordination behavior of this ligand is interesting since the free rotation of donor arms can give a different possible combination of coordination modes. Various possible coordination modes of **L**, as depicted in Scheme 3, can be observed for mononuclear complexes.

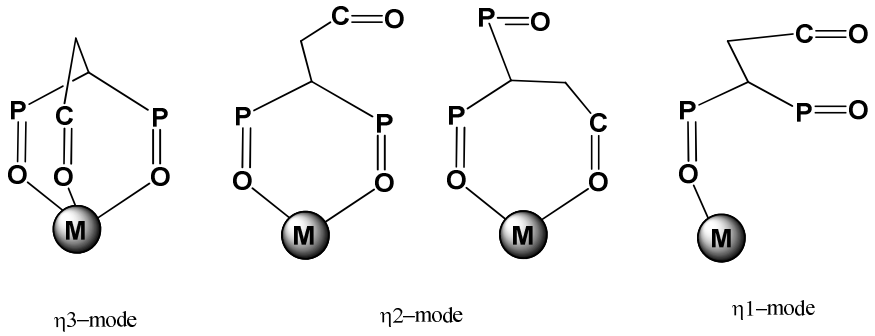

Scheme 3. Possible coordination modes of ligand **L** in mononuclear complexes

C(O)-Monodentate coordination is the least probable (not shown in the Scheme). Obviously, metal and composition of the complex affect the choice of coordination mode. The f-block element coordination chemistry of this scorpionate ligand was studied in order to understand its coordination behavior.

Mononuclear complex $[UO_2(\mathbf{L})(NO_3)_2]$ (**1**) was prepared by addition of 1 equivalent of $UO_2(NO_3)_2\cdot(H_2O)_6$ in acetonitrile to 1 equivalent of compound **L** in chloroform to form a bright yellow microcrystalline powder. Crystallization of an ethanolic solution of **1** when exposed to sunlight yielded a trace amount of a yellow product with structural analyses consistent with formula $[\{UO_2(NO_3)\mathbf{L}\}_2(\mu_2\text{-}O_2)]\cdot EtOH$ (**2**). The appearence of the bidenate peroxo $[O_2]^{2-}$ anion in uranyl nitrate solutions in the presence of atmospheric dioxygen is possible due to sunlight photolysis of EtOH.[14] The mechanism of this photolysis has been previously reported.[15]

Mononuclear bisligand complexes $[La(NO_3)_3\mathbf{L}_2]\cdot 2.33MeCN$ (**3**), $[Nd(NO_3)_3\mathbf{L}_2]\cdot 3MeCN$ (**4**), $[Nd(NO_2)_3\mathbf{L}_2]\cdot(NO_3)\cdot EtOH$ (**5**) and $[Lu(NO_3)_3\mathbf{L}_2]$ (**6**) isolated in pure state were obtained combining stoichiometric amounts of the ligand and the salts in a mixture of aprotic solvents followed by crystallization from the corresponding solvent.

The composition and structure of complexes in solid state were studied by elemental analysis, and IR spectroscopy. The structures of the crystal complexes **1**–**5** were also elucidated by X-ray diffraction.

2.2.1. X-ray structures

According to the data of single-crystal X-ray diffraction, compound **1** is the neutral mononuclear complex, where the uranium atom adopts the hexagonal bipyramidal geometry with one bidentate chelate ligand **L** and two bidentate nitrate anions situated in the equatorial plane and uranyl oxygen atoms in the apical positions (Fig. 2). The C=O group is oriented to the opposite direction with respect to the uranium atom).

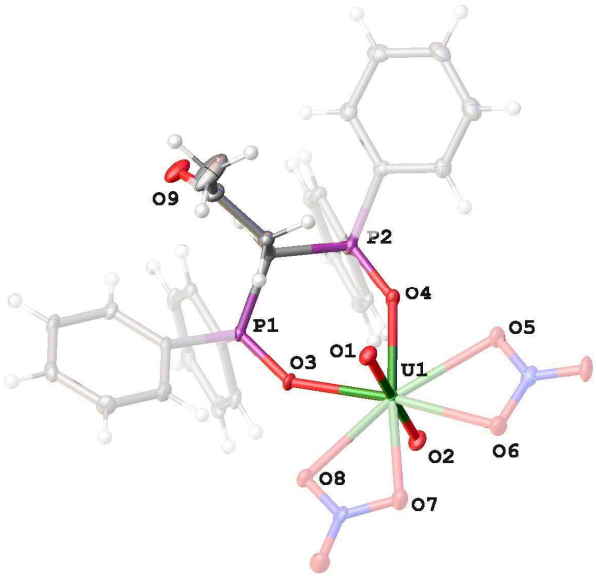

Fig. 2. General view of **1** given in representation of atoms in thermal ellipsoids drawn at p = 50 %

The absence of strong intermolecular interactions that involve oxygen atoms of the uranyl group, results in its linearity (the O1–U1–O2 angle is equal to 179.9(1)°) and similarity of the U=O distanses (1.760(2) and 1.761(2)Å) in **1**. In complex $[UO_2(NO_3)_2\mathbf{L'}]$ (**7**)[7] (where **L'** is $Ph_2P(O)CH_2P(O)Ph_2$), which has similar to **1** molecular structure, the U=O distances differ rather considerably, 1.781(11) and 1.768(11) Å, due to the presence of intermolecular C–H...O1 bonding. Complex **1** also involves intermolecular contacts C-H…O=C, with r(H...O) distances in them being virtually the same as in the structure of ligand (Fig. S2, ESI†).

Neutral dinuclear complex **2** (Fig. 3) contains only half of the complex in the asymmetric unit. The **L** acts as a bidentate chelate P(O),P(O)-ligand and the other equatorial positions of the uranium(VI) atom in **2** are occupied by the oxygen atoms of the bidentate chelate nitrate anion and the bridging bidenate peroxo anion.

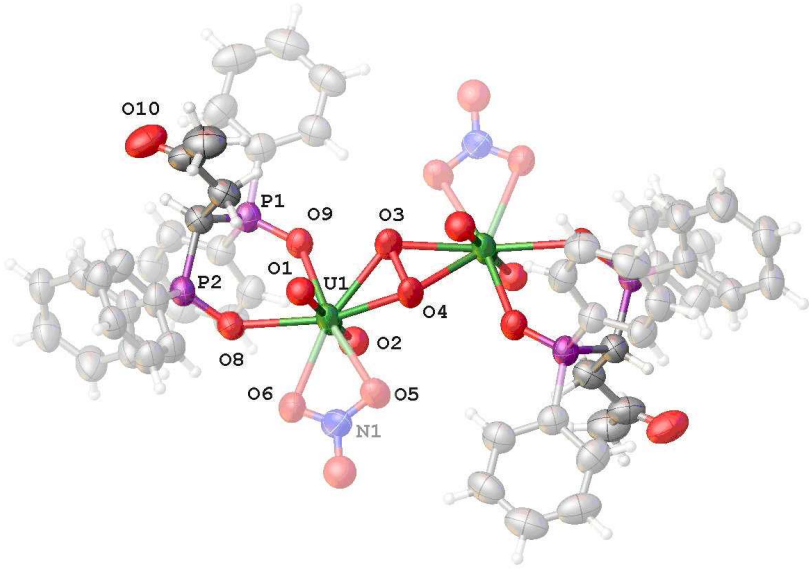

Fig. 3. General view of the **2** given in representation of atoms in thermal ellipsoids drawn at p = 50 %. Uranyl oxygen atoms, the peroxo group and an oxygen atom of the nitrate anion are disordered over two sites, and only one of the disordered components is depicted.

The resulting coordination polyhedron UO_8 adopts the hexagonal bipyramidal geometry with the uranyl oxygen atoms in apical positions. Two nitrates (and two **L** ligands) are *trans*-situated to each other in respect to the UO_2U species as it was previously observed in the complexes with similar $[\{UO_2(NO_3)X\}_2(\mu_2\text{-}O_2)]$ composition, where X is the bidentate chelate neutral ligand (X = tetraetylsuccinamide[16], 2,2'-bipyridyl[17] or 5,5'-dimethyl-2,2'-bipyridine[18]). The severe disorder of the peroxo, NO_3 and uranyl groups in **2** provides no possibility to analyze its molecular geometry in detail, the mutual disposition of the constituting moieties can still be assessed. Particularly, the equatorial planes of two UO_8 polyhedra connected through the peroxo anion are not parallel (the corresponding dihedral angle is *ca*. 21°), and deviate from planarity. Although this deviation is a rare case, it was previously reported for several peroxo complexes of uranium.[19]

Compounds **3** and **4** are isostructural, although the number of solvate molecules in their structures obtained from X-ray diffraction is not equal, probably due to the loss of solvent molecules in air. These contain only half of molecule in the asymmetric unit with Ln, N1 and O5 atoms situated on a two-fold rotation axis. The Ln atom in **3** and **4** coordinates three nitrate anions and two **L** ligands in the bidentate chelate mode to form the LnO_{10} coordination polyhedron (molecular view of **3** is given in Fig. 4 as an example). The nitrate anions are the T-shape situated in accord to the metal atom with the NLnN angles slightly deviating from 90° (the angle value is equal to 83.2(2) and 83.0(2)°) due to the electronic and steric effects of **L** ligands.

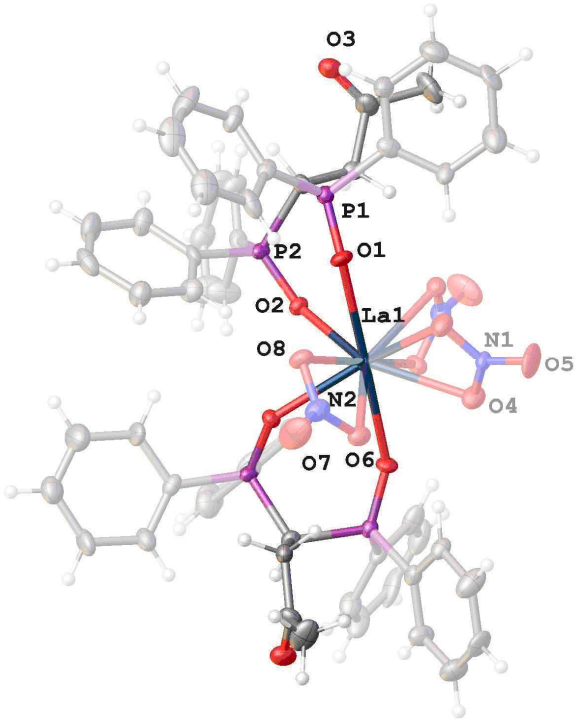

Fig. 4. General view of molecule **3** given in representation of atoms in thermal ellipsoids drawn at p = 50 %.

The resulting polyhedron forms a *pseudo*-capped trigonal prism with N1 atom in the capped position, if nitrate anions are regarded as one polyhedron vertex.

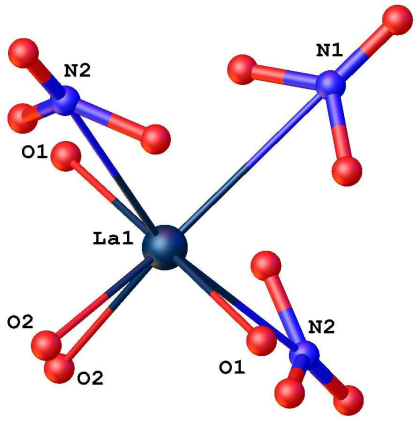

Fig. 5. Visualization of the *pseudo*-capped trigonal prismatic environment around La(III) in **3**.

In the closely related family of lanthanide nitrate complexes with **L'**, the compounds were characterized to be of the $[Ln(NO_3)_3(\mathbf{L'})_2]\cdot Solv$ (Ln = La, Solv = EtOH; Ln = Ce, Solv = acetone), $[Ln(NO_3)_2(H_2O)(\mathbf{L'})_2][Ln(NO_3)_2\mathbf{L'}]\cdot MeCN$ (Ln = Pr, Eu), $[Ln(NO_3)_2(H_2O)(\mathbf{L'})_2](NO_3)\cdot Solv$ (Ln = Nd, Gd, Solv = H_2O; Ln = Ho, Solv = EtOH) and $[Ln(NO_3)(\mathbf{L'})_3](NO_3)_2\cdot Solv$ (Ln = Gd, Yb; Ln = Gd, Solv = EtOH) composition.[6] Thus, although a lanthanide cation can coordinate up to four bis(diphenylphosphino)methane dioxide ligands (as in the structure of $[Eu(\mathbf{L'})_4](ClO_4)_3\cdot 2\ H_2O$)[20], nitrate anions compete with those for a place in lanthanide coordination sphere. The ratio Ln : NO_3 : **L'** (or **L**) = 1 : 3 : 2 is expected only for light elements (La, Ce); lanthanide contraction is accompanied by the decrease in this ratio as 1 : 2 : 2 (Ln = Pr – Ho) or as 1 : 1 : 3 (Ln = Gd – Yb). Thus, coordination isomerism is possible in this series.

Indeed, we succeeded to obtain from ethanol complex **5** for which the ratio Nd : NO_3 : **L** = 1 : 2 : 2 (Fig. 6).

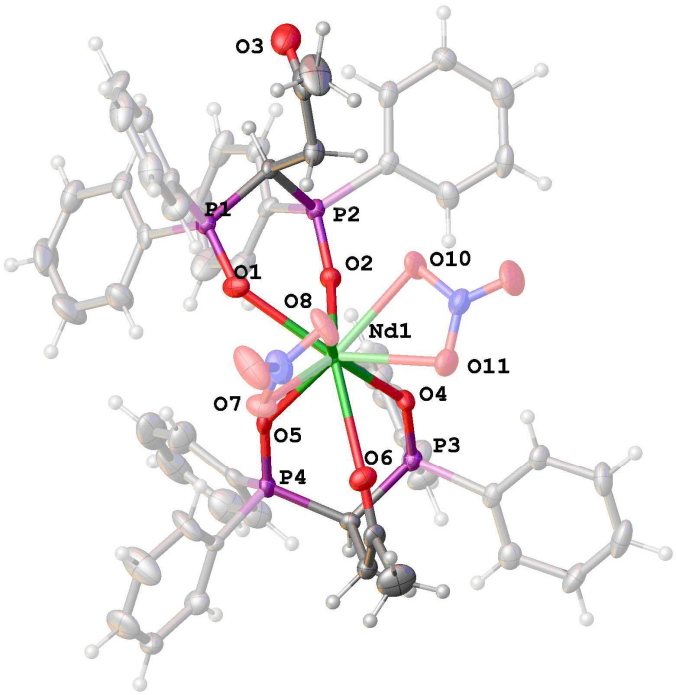

Fig. 6. General view of complex cation $[Nd(NO_3)_2\mathbf{L}_2]^+$ in the structure of **5** given in representation of atoms in thermal ellipsoids drawn at p = 50 %.

It contains two **L** ligands in both the P(O),P(O)-bidentate and tridentate coordination modes, and only two nitrate anions coordinated by the neodymium atom. The NdO_9 polyhedron adopts the tricapped trigonal prismatic geometry (Fig. 7).

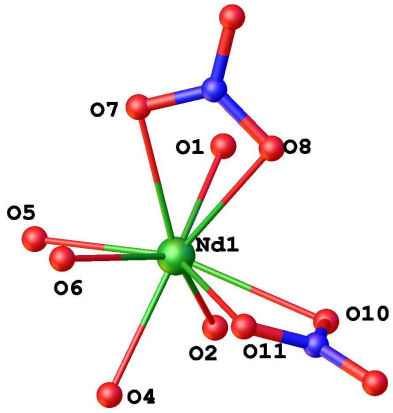

Fig. 7. Visualization of the tricapped trigonal prismatic environment around Nd(III) in **5**.

For compounds **3–5**, the Ln – O(L) bond distances are shorter than those for the Ln–O(nitrate) bonds (Table 2); and the latter bonds are typically alternated. In **5**, the Nd–O(C) bond is the longest, and, hence, the weakest among coordination bonds. Lanthanide contraction for isostructural compounds **3** and **4** is expressed as shortening of respective coordination bonds.

Table 2. Selected bond distances (Å) in complexes **3–5**

Bond	**3** (La)	**4** (Nd)	**5** (Nd)
Ln–O1(**L**)	2.541(6)	2.5016(9)	2.462(5)
Ln–O2(**L**)	2.501(7)	2.4573(9)	2.410(4)
Ln–O4(**L**)			2.389(4)
Ln–O5(**L**)			2.405(5)
Ln–O(C)			2.656(5)
C=O (free)	1.202(13)	1.214(2)	1.217(9)
C=O (coordinated)			1.222(7)
Ln–O(nitrate)	2.599(8) – 2.653(6)	2.555(1) – 2.609(1)	2.536(5) – 2.551(4)
P1–O1	1.491(7)	1.4957(9)	1.514(5)
P2–O2	1.504(7)	1.5010(9)	1.492(4)
P3–O4			1.496(4)
P4–O5			1.505(4)

The coordination of phosphoryl and acetyl groups does not affect the lengths of the P=O and C=O bonds, although the oxygen atom of the longest P=O bond in **5** is involved in O–H...O hydrogen bonding with ethanol molecule (r(O...O) = 3.844(8) Å, ∟(OHO) = 165.9°) (Fig. S4, ESI†). With an exception of one ligand in **5**, the acetyl group of **L** in complexes **1–5** is involved in the CH...O=C intra- and intermolecular bonding (Figs. S1–S4, ESI†). The most significant noncovalent CH…O=C interactions are observed in complexes **3**, **4** with shortest O…H distances 2.53–2.55 Å and corresponding value of the CHO angle ~145° (Fig. S3, ESI†). In our opinion, the presence of an uncoordinated acetyl group available for complex...solvate hydrogen bonding can be the reason of enhanced extraction ability of the **L** as compared with the **L'**. To reveal crystal packing effect on IR spectra of **1**, **3–5** in solid state, we analyzed the closest environment of these complexes. The O–H...O bond in **5** should affect the P=O vibrations. Moreover, one can expect the effect of weak intermolecular C–H...O=C interactions (for **3** and **4**) on acetyl group vibration.

Along with numerous C–H...O intramolecular bonds, intramolecular π-bonding can be suggested for **1–5** that could affect the stability of complexes. These are analyzed in the next Section.

2.2.2. *AIM analysis for complexes 1–5*

It is well known that the topological analysis of electron density (ED) ρ(**r**) according to Bader's "Atom in Molecules" theory (AIM)[21] derived from *ab initio* calculations in conjunction with Espinosa's correlation (E_{cont}= –½ V(**r**))[22] makes it possible to estimate the interaction energy (E_{cont}) with sufficient accuracy.[23]

To evaluate π-stacking energy, the topological analysis of ED for complexes **1**–**5** was performed using X-ray geometry data on DFT level of theory. Unlike the neutral compounds **1**–**4**, complex **5** is both ionic and paramagnetic, for which convergence of SCF equations has not been achieved in spite of our effort to change basis set for neodymium atom or convergence algorithms. We calculated this value for model free ligands being in geometrical configuration like as in X-ray structure of complex **5**.

The AIM results are presented in Fig. 8 and in Table 3. Molecular graphs of complexes **1**–**5** exhibit various sets of bond critical points (BCP) and bond paths corresponding to different types of π-stacking interactions.

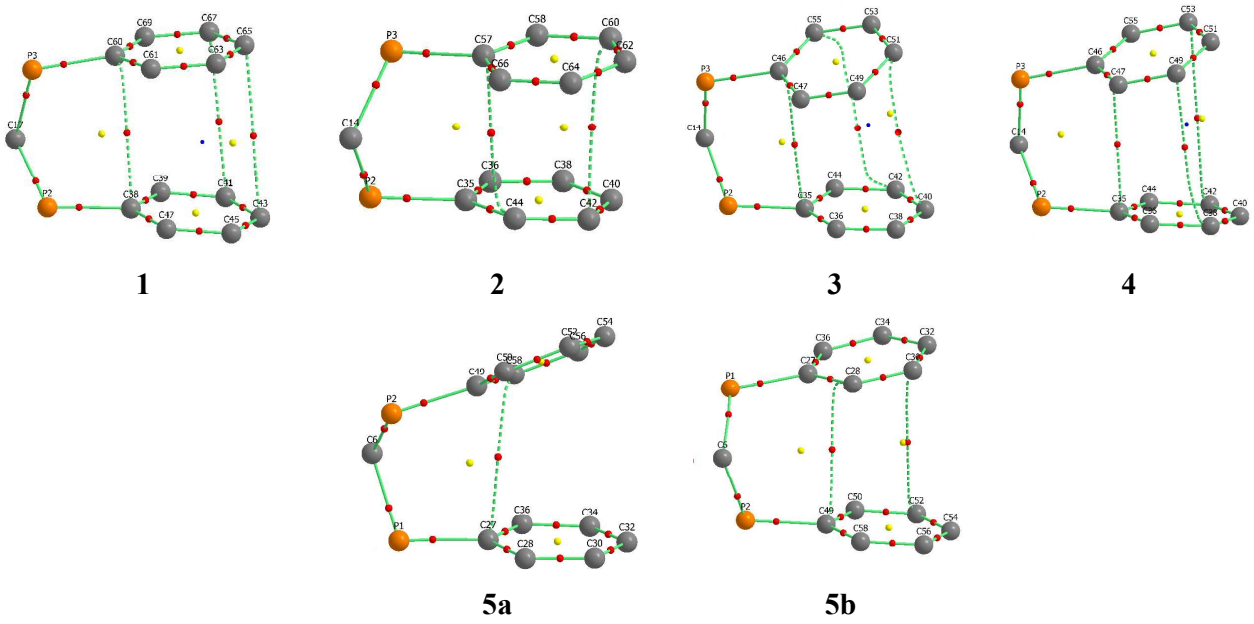

Fig. 8. The fragments of QTAIM graphs for complexes **1**–**5** exhibiting π-stacking interactions in these complexes (**a**, **b** – tri- and bidentate ligand coordination in complex **5**). Hydrogen atoms are omitted for clarity. Color codes for the atoms: orange (P), grey (C). The π-stacking bond paths are shown as green dotted lines; BCPs (3;-1) are red, ring (3;+1) critical points are yellow, and cage (3;+3) critical points are blue.

The change in the parameters of intramolecular π-stacking interactions (Table 3) for complexes **1**–**5** depends on mutual geometric configuration of benzene rings (Table 4). The larger the distance between the rings and corresponding interplanar angle the smaller interaction energy value. The topology of molecular graphs is affected by the parallel shift of two benzene rings (*e.g.* for **2** and **3** complexes), hence, the number of bond paths and overall interaction energy decrease. The most pronounced stacking interaction is observed in complex **1** (interplane distances are 3.505 Å). The total energy of π-stackings in **1**–**5** amounts to 2.3, 4.0, 2.8, 3.2 and 2.3 kcal/mol respectively. Interestingly, the ligands in **5** exhibit different coordination: bi- and tridentate fashion. This leads to different molecular graphs in π-stacking interaction fragment (**5a** and **5b** at Fig. 8), containing one and two bond paths for tridentate and bidentate ligands, respectively. Thus, the π -stacking interaction in tridentate ligand (**5a**) is the weakest (only 0.8 kcal/mol) in the series studied.

The obtained π-stacking interaction energy values are close to those for intramolecular π-stacking in Co(III) complex[24] of about 1–3 kcal/mol and to those for intramolecular interligand π-stacking interaction in Lu(III) complexes[25] of about 1.9–3.3 kcal/mol.

Table 3. Topological parameters (QTAIM) in the critical points (3,–1) for π-stacking interactions in complexes **1**–**4** and complex cation **5** at PBE0/6-311+G** level.

Complex	BCP (3;-1)	ρ(**r**), a.u.	$\nabla^2\rho$(**r**), a.u.	V(**r**), a.u.	E_{cont}, kcal/mol	ΣE_{cont}, kcal/mol
1	C38–C60	+0.008252	+0.022976	–0.003955	1.3	2.3
	C45–C63	+0.003848	+0.010428	–0.001669	0.5	
	C43–C65	+0.004001	+0.010002	–0.001642	0.5	
2	C44–C57	+0.008598	+0.024180	–0.003988	1.3	2.0
	C42–C60	+0.005467	+0.014297	–0.002330	0.7	
3	C35–C46	+0.006458	+0.018423	–0.002927	0.9	1.4
	C40–C51	+0.001889	+0.005211	–0.000794	0.3	
	C42–C55	+0.001672	+0.004601	–0.000699	0.2	
4	C35–C47	+0.006593	+0.018433	–0.002946	0.9	1.6
	C39–C49	+0.003703	+0.009296	–0.001505	0.5	
	C42–C52	+0.001324	+0.003886	–0.000592	0.2	
5	C27–C58[a]	+0.005527[a]	+0.015985[a]	–0.002511[a]	0.8[a]	0.8[a]
	C28–C49[b]	+0.007119	+0.019434	–0.003138	1.0[b]	1.5[b]
	C30–C52[b]	+0.003728	+0.009775	–0.001713	0.5[b]	

[a] for tridentate ligand coordination;
[b] for bidentate ligand coordination.

Table 4. Geometrical parameters of π-stacking[a] for complexes **1**–**4** and complex cation **5**

	1	**2**	**3**	**4**	**5**[b]	**5**[c]
M	U	U	La	Nd	Nd	Nd
d, Å	3.505	3.710	3.816	3.849	4.644	3.831
l, Å	3.505	3.760	3.827	3.841	4.123	3.825
β, º	9.25	8.03	23.15	24.21	29.82	13.76

[a] d is the average distance between the contacting planes; l is the centroid-centroid distance; β is the average dihedral angle between the planes of contacting fragments.
[b] for tridentate ligand coordination;
[c] for bidentate ligand coordination.

The analysis of literature data on the structure of crystalline complexes of methylenediphosphine dioxide **L'** with uranyl nitrate $[UO_2(NO_3)_2\mathbf{L'}]$ (**7**)[7] and lanthanum nitrate $[La(NO_3)_3(\mathbf{L'})_2]\cdot EtOH$ (**8**)[6] also indicates π-stacking in the molecules of coordinated ligand **L'**. However, the stacking interaction in the complexes of unmodified ligand **L'** are weaker than in complexes of **L** at the same chelate coordination. Thus, the dihedral angles between contacting planes in uranyl complexes **1** and **7** are 9.25° and 13.17°, respectively, while the distances between centroids are 3.505 and 3.736 Å, respectively. In the lanthanum nitrate complexes with **L** and **L'**, **3** and **8**, the noted angles are 23.1 and 12.17, 12.66°, while the distances are 3.816 and 3.940, 4.079 Å (the contacting fragments in complex **8** are skewed toward each other).

Thus, π-stacking interaction between two Ph substituents at phosphorus atom is observed in molecule(s) of coordinated ligand **L** for all crystalline complexes **1**–**5.** The highest energy of π-stacking interaction was found for bisligand uranyl complex **2**. The change of ligand denticity

from P(O),P(O)-bidentate to P(O),P(O),C(O)-tridentate almost doubly decreases the energy of π-stacking interaction (see Table 3).

The above discourse deals with the stabilization of complexes in a crystal, but situation may change in solutions. Solvent nature is known to affect considerably aromatic π-stacking interaction. However, π-stacking interaction retains as a rule in dipolar aprotic solvents.[26]

2.2.3. IR spectroscopy characterization

The X-ray structures were compared with the IR spectra of the same complexes (Table 5).The formation of P=O→M coordination bond results in the shift of ν(P=O) band in IR spectra of crystalline complexes **1**, **3**–**6** by ~ 40 cm^{-1} to the low frequency region with respect to the band of free ligand (Table 5), which is slightly lower than in similar complexes of phosphoryl-containing ligands (Δν(P=O) ~ 65cm^{-1} for UO_2 complexes[7,27], and ~ 50 cm^{-1} for Ln complexes[28]). The spectrum of complex **5**, along with ν(P=O) band at 1160 cm^{-1}, also displays a band at 1150 cm^{-1} responsible for vibrations of coordinated P=O group participating in formation of supplementary weak H bond with solvate EtOH molecule. The formation of C=O→M coordination bond in complex **5** causes the shift of ν(C=O) band to the low-frequency region but only by 9 cm^{-1} relative to the band of free ligand, whereas usually coordination of C=O to cation leads to the shift of 20–25 cm^{-1} for lanthanide complexes and 20–60 cm^{-1} for UO_2 complexes.[16,27b,29] The band of uncoordinated C=O group in the spectrum of crystalline complex **1** is observed[30] at the same frequency as in the spectrum of free ligand (Table 5). In the isostructural complexes of La and Nd (**3** and **4**, respectively), the shift of ν(C=O) band by 4–3 cm^{-1} corresponds to vibrations of C=O group involved into weak intra- and intermolecular CH…O=C interactions (Table 5). The spectrum of crystalline complex **5** exhibits a band of free C=O group that does not involved into supplementary interactions at 1722 cm^{-1}.

The IR spectra of complexes **1**, **3**–**6** show absorption bands of bidentate nitrate ions at ~ 1500 cm^{-1} for ν(N=O), and ~ 1300 cm^{-1} for $\nu_{as}(NO_2)$ (Table 5). Full details of the nitrate bands are shown in the Table S1 (ESI†). In contrast to other complexes, X-ray structure **5** includes, along with bidentate coordinated nitrate ions, outer-sphere "free" nitrate ion involved in many weak CH…ON interactions. The symmetry of an uncoordinated nitrate ion is known to be violated on weak interactions in crystal or contact ion pairs (CIP) on account of cation-anion interaction that causes strong splitting of $\nu_E(NO_3)$ vibration.[31] As should be expected, the spectrum of crystalline compound **5** shows no absorption of free nitrate ion, which usually appears as a narrow intense band at ~1370 cm^{-1},[31] but displays a wide absorption in the region 1300–1500 cm^{-1} with several submaxima at 1338, 1384, and 1396 cm^{-1}.

According to the data of elemental analysis and X-ray crystallography, complexes **3** and **4** contain solvate acetonitrile, but the IR spectra of **3** and **4** exhibit no absorption of CN group[32]. The IR spectra of **5** show bands typical for outer-sphere ethanol molecules in the region of ~ 3400 cm^{-1}.

We failed to prepare complex **6** in a crystal state. But elemental analysis and IR spectra allows us to suppose unambiguously that one ligand molecule in bisligand complex **6** is coordinated in P(O),P(O)-bidentate mode, while another molecule has P(O)-monodentate coordination. The IR spectrum of solid complex **6** (Table 5) shows bands of free P=O and C=O groups at 1185 and 1721 cm^{-1} along with the band of coordinated P=O group at 1161 cm^{-1}. The strong broad IR bands of bidentate NO_3 groups are detected at 1494, 1310 and 1030 cm^{-1}. In the region of 3200–3400 cm^{-1} the band of metal-coordinated water (typically at ~3200 cm^{-1}) is absent. In accordance with these data, one can suppose that compound **6** most likely has the structure of neutral mononuclear complex [Lu{P(O),P(O)-**L**}{P(O)-**L**)(O,O-NO_3)$_3$)], and coordination number of lutetium is nine.

Thus, lanthanide contraction is observed for the structure of the studied neutral complexes of ligand **L**. The coordination number (CN) of light lanthanides (La and Nd) in complexes **3**, **4**, [Ln{P(O),P(O)-**L**}$_2$(NO_3)$_3$], equals to ten, while CN of lutetium in complex **6**, [Lu{P(O),P(O)-L}{P(O)-**L**)(O,O-NO_3)$_3$)], is nine.

Table 5. Selected IR (ν, cm^{-1}) and $^{31}P\{^{1}H\}$ NMR spectroscopic data for the ligand **L** and its complexes **1, 3–6** in solid state and in solution (0.01 M)

Com-pound	Sample	ν(P=O)	ν(C=O)	ν(N=O)	$\nu_{as}(NO_2)$	δ_P ($W_{½}$)[a]
L	cryst.	1202,1182	1720			
	in CD_3CN[b]	1207,1200	1720			29.8 (0.01)
	in $CDCl_3$[b]	1199sh,1181	1719			31.2 (0.03)
1	cryst.	1166	1720	1518	1308,1282	
	in CD_3CN[c]	1195,1165	1719	1523	1290,1273	46.2 (0.02)
	in $CDCl_3$[c]	1171	1718	1526	1283	44.4 (0.03)
3	cryst.	1166	1716[d]	1458	1313	
	in CD_3CN	1170	1720	1455	1318	37.0 (0.08)
	in $CDCl_3$	1173	1713	1450	1319	36.0 (0.7)
4	cryst.	1164 br	1717[d]	1465	1306	
	in CD_3CN	1162	1709,1720	1469	1308	86 (2.5)
	in $CDCl_3$	1173, 1162	1712	1460	1313	86(5),70(6)
5	cryst.[e]	1160,1150[f]	1711,1722sh	1503,1465	1285,1300	
	in CD_3CN	1162	1709,1720	1469	1308	86 (2.5)
	in $CDCl_3$	1174,1162	1712	1460	1313	86(5),70(6)
6	solid	1185, 1161	1721	1494,1518sh	1310	
	in CD_3CN[g]	1189, 1159	1723	1527,1512	1293	42.4 (0.5)
	in $CDCl_3$	1195, 1174, 1162	1715	1490	1310	40.3 (0.5)

[a] The band width at half-height (in ppm).
[b] c = 0.02 M
[c] Saturated solution, c ~ 0.003 M.
[d] Non-covalent CH…O=C interaction (see Section 2.2.1).
[e] A wide absorption in the region 1300–1400 cm^{-1} (weak CH…ON interaction of "free" nitrate – see Section 2.2.3).
[f] Weak OH…O bonding between coordinated P=O and EtOH (see Section 2.2.1).
[g] The strong band at 1356 cm^{-1} – $\nu_E(NO_3)$ (see Section 2.3.1).

2.3. Solution state characterizations

The structure of the complexes in acetonitrile (AN) and chloroform solutions was studied by IR and multinuclear NMR spectroscopy. We were interested to study the effect of solvent nature on the structure of complexes and ligand **L** coordination mode. The parameters of IR and ^{31}P, ^{1}H, and ^{13}C NMR spectra for the complexes **1**, **3–6** in comparison with the data for the free ligand **L** are given in Tables 5–7 (see also Figs. S5–S12, ESI†).

The coordination of P=O groups is reliably determined by the NMR spectra of compounds **1**, **3–6**. The signals of phosphorus nuclei as well as protons and carbon nuclei of neighboring groups exhibit expected shifts (Tables 5–7) close to that for known complexes of akin phosphoryl-containing ligands[8a,c,27a,b,28]. The coordination of phosphoryl-containing ligand with UO_2(II), La(III), Lu(III), and Nd(III) cations causes downfield shift of signals of phosphorus nuclei by 5–60 ppm, while signals of protons and carbon nuclei of neighboring groups are shifted upfield; the signals of paramagnetic neodymium complex show considerable broadening. The participation of C=O group in coordination appears in ^{13}C and ^{1}H NMR spectra as a downfield shift of carbon signals of C=O group as well as carbon and proton nuclei signals of neighboring CH_3 and CH_2 groups relative to free ligand signals (Tables 6, 7), however, the value of these shifts in the spectra of complexes of ligand **L** is lesser than that of corresponding complexes for the majority of carbonyl ligands (for example[16,27b,29b]).

Table 6. Selected ^{1}H and ^{13}C NMR data for the ligand **L** and its complexes **1**, **3**–**6**[a] in CD_3CN (0.01 M) at 25°C

Com-	δ ^{1}H			δ ^{13}C			
pound	$C\underline{H}_3$	$C\underline{H}_2$	$C\underline{H}$	$\underline{C}H_3$	$\underline{C}H$	$\underline{C}H_2$	C=O
L[b]	1.55 s	2.98 dt	4.46 tt	28.28 s	35.61 t	38.13 s	204.04 t
1[c]	1.30 br s	2.98 dt	5.19 br t	28.15 s	32.64 t	36.94 s	202.6 br s
3	1.47 s	3.19dt	4.67 tt	28.18 s	32.00 s	37.81 s	203.3 br s
4	1.10 s	4.1 br s	– [d]	28.30 s	29.9 br s	39.3 br s	205.4 br s
6	1.44 s	3.10 dt	4.93 tt	28.10 s	31.72 t	37.66 s	202.8 br s

[a] Spectra of complexes **4** and **5** are identical.
[b] 0.02 M solution.
[c] Saturated solution, c ~ 0.003 M.
[d] Not observed.

Table 7. Selected ^{1}H and ^{13}C NMR data for the ligand **L** and its complexes **1**, **3**, and **6** in $CDCl_3$ (0.01 M) at 25°C

Com-	δ ^{1}H			δ ^{13}C			
pound	$C\underline{H}_3$	$C\underline{H}_2$	$C\underline{H}$	$\underline{C}H_3$	$\underline{C}H$	$\underline{C}H_2$	$\underline{C}$=O
L[a]	1.54 s	2.94 dt	4.45 tt	28.81 s	36.73 t	38.70 s	203.84 t
1[b]	1.38 s	2.84 dt	4.95 br t	28.83 s	37.72 br s	31.93 s	203.4 br s
3	1.62 s	3.36 t	4.63 br s	29.17 s	32.43 br s	39.15 br s	206.2 br s
6	1.61 s	3.28 t	5.04 br s	28.98 s	33.05 t	39.81 s	205.7 br s

[a] 0.02 M solution.
[b] Saturated solution, c ~ 0.003 M.

2.3.1. Acetonitrile solutions

Uranyl complex **1** is poorly soluble in AN. The IR spectrum of its saturated solution shows a band of coordinated P=O group at 1165 cm^{-1} as well as the bands of free P=O and C=O groups at 1195 and 1719 cm^{-1}. The bands of nitrato groups virtually retain as compared with the spectrum of crystalline sample (Table 5). One can suppose that the ligand adopts P(O)-monodentate coordination in AN solution, the coordination sphere of cation is supplemented by solvent molecule, while neutral complex has $[UO_2\{P(O)\text{-}\mathbf{L}\}(OO\text{-}NO_3)_2 \cdot MeCN]$ structure.

The data of NMR spectra of compound **1** (Tables 5, 6) agree well with the proposed structure. Certain signals in the spectra are broadened. ^{31}P NMR spectrum displays only one slightly broadened signal, which seems to be explained by fast exchange processes. The signal is shifted downfield relative to the signal of free ligand by 16.4 ppm. In the ^{13}C NMR spectrum, the carbon signals of C=O, $\underline{C}H_3$, and $\underline{C}H_2$ groups are upfield shifted (Table 6). The largest upfield shift (–2.97 ppm) is observed for the broadened signal of $\underline{C}H$ group, which is typical when P=O group is involved into coordination. The corresponding effects are observed in the ^{1}H NMR spectrum (Table 6).

The lanthanide complexes are well soluble in AN, chloroform, and methanol. According to IR spectral data, the structure of crystal lanthanum complex **3** retains in AN solution (Scheme 4). The bands of P=O, C=O groups and nitrate ions have expected frequencies (Table 5), complicated pattern in the spectrum of crystalline sample caused by supplementary weak interactions

disappears. Bisligand complex **3** in AN solution, like in crystal state, seems to remain neutral [La{P(O),P(O)-**L**}$_2$(OO-NO_3)$_3$], CN of lanthanum is ten.

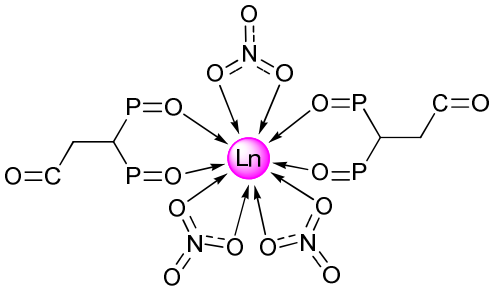

Scheme 4. Complex **3** (Ln = La) in crystal state and in AN solution, and complex **4** (Ln = Nd) in crystal state.

NMR spectral data for compound **3** (Tables 5, 6) agree well with the proposed structure (Scheme 4). ^{31}P NMR spectra display a sole narrow signal ($W_{½}$ = 0.08 ppm) of phosphorus nuclei downfield shifted by 7.2 ppm from its position in the free ligand. The signals of indicator groups (C=O, $\underline{C}H_3$, and $\underline{C}H_2$) in ^{13}C NMR are shifted upfield, which indicates the lack of coordination of C=O group. The largest shift in ^{13}C NMR spectrum is observed for the signals of CH groups (–3.61 ppm). The shifts in ^{1}H NMR spectrum are less considerable (Table 6), the protons of CH_3 group show the least shift (–0.08 ppm), while the protons of CH и CH_2 groups exhibit the largest shift (0.21 ppm). A fine signal structure is observed in the spectrum.

IR and NMR spectra of neodymium complexes **4** and **5** in AN solution are identical (Tables 5, 6). The complications in the IR spectrum of crystalline sample of **5** caused by weak interactions in crystal disappear in solution spectrum. The main analytical bands have close positions to those in the spectrum of crystalline **5** (Table 5). We observed no band of vibrations of free nitrate ions expected at ~1360 cm^{-1}. Both complexes seem to be present in AN solution as contact ion pair [Nd{P(O),P(O)-**L**}{P(O),P(O),C(O)-**L**}(OO-NO_3)$_2$]$^+$·$(NO_3)^-$, CN of neodymium is nine (Scheme 5).

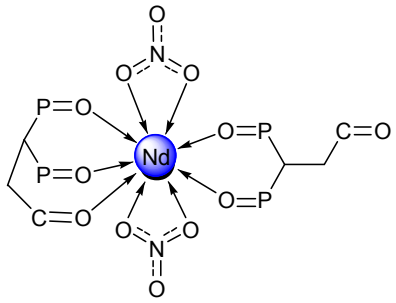

Scheme 5. Complex cation of compounds **4**, **5** in AN solution

The sole signal in ^{31}P NMR spectrum of neodymium complex **4** in AN at 86 ppm (analysis of NMR spectra is given for one complex because the spectra of solutions of **4** and **5** are identical) is considerably broadened ($W_{½}$ = 2.5 ppm). In ^{1}H NMR spectrum, the proton signals of all groups except for CH_3 and CH_2 are also broadened, no signal of CH protons is observed probably due to both paramagnetic properties of neodymium cation and dynamic equilibria in solution. The signals of CH_3 and CH_2 groups are from their positions in the free ligand by – 0.14 and 1.12 ppm, respectively. ^{13}C NMR spectrum exhibits one set of signals, it seems to correspond to fast dynamic equilibrium of several complex species. Alterations of chemical shifts in ^{13}C NMR spectrum agree well with the suggested complex structure (Scheme 5).

According to IR spectroscopy, the structure of lutetium complex **6** in AN solution and solid state differs. The main difference is the emergence of strong vibrational band of free nitrate ion at 1356 cm^{-1}. Furthermore, strong bands of bidentate coordinated nitrato groups are detected at

1527, 1512, and 1293 cm^{-1}. Vibration bands of P=O and C=O groups are observed at almost the same frequencies as in the spectrum of solid sample (Table 5). Obviously, ligand molecules retain the same coordination as in the solid complex. In accordance with these data, one can suppose that complex **6** in AN solution exists as either solvent-separated ion pair (SSIP) or cationic complex $[Lu\{P(O),P(O)\text{-}\mathbf{L}\}\{P(O)\text{-}\mathbf{L}\}(OO\text{-}NO_3)_2]^+$ and free nitrate ion. In this case, the CN of lutetium should be equal to seven. Both the forms, most probably, are in equilibrium. Since CN of lutetium of eight and nine[33] are more typical, one can suppose that remaining sites in lutetium coordination sphere will be occupied by solvent molecules $[Lu\{P(O),P(O)\text{-}L\}\{P(O)\text{-}L\}(OO\text{-}NO_3)_2(MeCN)_m]^+\cdot(NO_3)^-$ (Scheme 6). Complex species with coordinated solvent molecules are most likely to be involved in dynamic equilibria with species containing no coordinated solvent molecules to cause signal broadening in ^{31}P NMR spectrum.

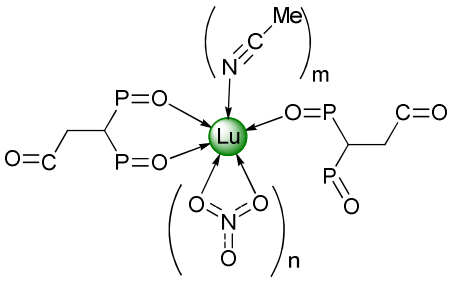

Scheme 6. Complex **6** in solid state (n = 3, m = 0), and complex cation of compound **6** (n = 2, m = 1 or 2) in AN solution

The data of NMR spectra (Tables 5, 6) agree well with the supposed structure (Scheme 6). The ^{31}P NMR shows the sole broadened signal of phosphorus nuclei, which seems to be explained by fast exchange processes. The signal is downfield shifted by 12.6 ppm relative to free ligand signal. ^1H and ^{13}C NMR spectra display expected changes.

Thus, in AN solutions, lanthanum (**3**) and neodymium (**5**) complexes retain the structure revealed in the crystal. The structure of uranyl (**1**), neodymium (**4**), and lutetium (**6**) complexes changes in solution. In the studied complexes in AN solutions, the scorpionate ligand **L** show three coordination modes: P(O)-monodentate, chelate P(O),P(O)-bidentate, and P(O),P(O),C(O)-tridentate. Uranyl (**1**) and lanthanum (**3**) complexes in AN solutions are neutral, whereas neodymium (**4**, **5**) and lutetium (**6**) complexes are cationic.

2.3.2. Chloroform solutions

In chloroform solutions, only uranyl complex **1** retains the structure revealed in the crystal, the structure of all other lanthanide complexes changes.

Uranyl complex **1** is relatively poor soluble in chloroform (~ 0.003 M), however, it is much better soluble (> = 0.02 M) in solution containing 3 equiv. of ligand **L**. The ^{31}P NMR spectra of the 3:1 mixture showed at least 3 broad peaks at 45.9, 45.3 and 45.0 and one peak at 31.6 ppm with inegral intensity ratio ~ 2:3, which indicates the presence of complex species of different stoichiometry containing both P(O)- and P(O),P(O)-coordinated ligand molecules. The position of analytical bands in the IR spectrum of solution of compound **1** slightly differs as compared with the spectrum of crystalline sample (Table 5). The ^{31}P NMR spectrum shows a singlet at 44.4 ppm. The ^1H NMR spectrum of complex **1** shows that the CH resonance is shifted downfield by *ca*. –0.5 ppm with respect to the free ligand, the CH_3 resonance is shifted downfield by ca. –0.10 and –0.25 ppm (Table 7). The proton signal of the CH group is broadened. The carbon signals of indicator groups C=O, $\underline{C}H$, and $\underline{C}H_2$ in ^{13}C NMR spectrum are shifted upfield relative to free ligand signals (Table 7). These changes agree well with chelating P(O),P(O)-mode of ligand coordination. The neutral uranyl complex in chloroform solution has structure $[UO_2\{P(O),P(O)\text{-}\mathbf{L}\}(OO\text{-}NO_3)_2]$.

The structure of lanthanum complex **3** in chloroform solution according to the data of IR spectroscopy (Table 5) differs from that in the crystal and AN solution. Both ligand molecules in

complex **3** are coordinated in P(O),P(O),C(O)-tridentate mode. The bands of coordinated P=O and C=O groups are observed at 1173 and 1713 cm^{-1}. The bands at 1450 and 1319 cm^{-1} correspond to bidentately coordinated nitrato groups. Taking into account typical lanthanum coordination number of ten, one can suppose that complex **3** in chloroform solution is present as a contact ion pair $[La\{P(O),P(O),C(O)\text{-}\mathbf{L}\}_2(OO\text{-}NO_3)_2]^+\cdot(NO_3)^-$ (Scheme 7).

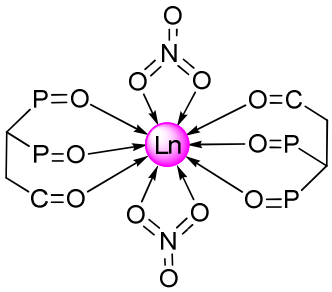

Scheme 7. Complex cations compounds **3** (Ln = La) and **4**, **5** (Ln = La, Nd) in $CDCl_3$ solutions

The data of NMR spectra (Tables 5–7) agree well with the proposed structure. The ^{31}P NMR spectrum shows a sole broadened phosphorus signal at 36.0 ppm shifted from free ligand signal by 4.8 ppm. The ^{1}H NMR spectrum displays the signals of CH_3, CH_2, and CH groups downfield shifted relative to free ligand signal, the signals of two latter groups are broadened. The largest shift is observed for the protons of the CH_2 group (0.42 ppm), whereas the signals of CH_3 and CH groups are shifted by 0.08 and 0.18 ppm. The ^{13}C NMR spectrum of complex **3** in chloroform solution exhibits considerably broadened signals of $\underline{C}H_2$, $\underline{C}H$, and $\underline{C}$=O groups. The signals of $\underline{C}H$ and $\underline{C}$=O groups have the largest shift relative to free ligand signal: –4.3 and 2.4 ppm, respectively. The signals of $\underline{C}H_3$ and $\underline{C}H_2$ groups are shifted much lesser: 0.36 and 0.5 ppm. Signal broadening observed for the all NMR spectra of chloroform solutions of **3** indicates relatively fast on NMR time scale equilibria with participation of other types of complexes (for example $[La\{P(O),P(O)\text{-}\mathbf{L}\}_2(OO\text{-}NO_3)_3]$ and similar species).

The spectra of neodymium complexes **4** and **5** in chloroform are identical except for the bands of solvate ethanol at 3683 and 3622 cm^{-1} in the spectrum of **5**. According to IR data, the structure of complexes **4** and **5** in chloroform solutions differs from that revealed in the crystal and AN solution. In chloroform solution, both ligand molecules are coordinated in tridentate mode. The bands of coordinated P=O groups are detected at 1173 and 1162 cm^{-1}, those of coordinated C=O groups are observed at 1712 cm^{-1}. The bands at 1460 and 1313 cm^{-1} correspond to nitrato group vibrations. One can suppose that the neodymium bisligand complex in chloroform solution has the same structure as lanthanum complex **3**: $[Nd\{P(O),P(O),C(O)\text{-}\mathbf{L}\}_2(OO\text{-}NO_3)_2]^+\cdot(NO_3)^-$ (Scheme 7). The CN of neodymium is ten.

Paramagnetic properties of neodymium hamper the use of NMR spectroscopy to study the structure of Nd complexes. However, signal broadening in NMR spectra of complexes **4** and **5** is much larger than that observed for neodymium nitrate complexes with other phosphoryl-containing ligands[28b-e,34]. Thus, the ^{1}H NMR spectrum of complex **4**, the signals of all protons either considerably broadened or not detected at all. The ^{31}P NMR spectrum shows two broad signals at 86 and 70 ppm ($W_{1/2}$ = 5 and 6 ppm, respectively) with approximate ratio 8:1 (Table 5), which indicates the presence of equilibrium in solution of the studied complex. One can suppose that dynamic equilibria involve structural isomers with different ligand coordination modes, species different in the number of coordinated nitrato groups or ligand molecules, intermolecular exchange processes, etc. ^{13}C NMR spectrum could not be interpreted correctly because of the presence of additional signals.

The IR spectrum of lutetium complex **6** chloroform solution shows the bands of coordinated P=O groups at 1162 и 1173 cm^{-1} and a shoulder at 1195 cm^{-1} responsible for vibrations of free P=O group. The band at 1715 cm^{-1} slightly shifted relative to free ligand band (1719 cm^{-1}) corresponds to vibrations of C=O group. A wide absorption at 3200 cm^{-1} corresponds

to vibrations of coordinated water. The bands at 1490 and 1310 cm^{-1} are consistent with bidentately coordinated nitrato groups. In accordance with these data, one can suppose that complex **6** in chloroform solution exists as an ion pair. Both ligand molecules are coordinated through one and two phosphoryl groups, however, it is rather difficult to determine interaction mode for the C=O groups. One can suppose that both C=O groups form H-bonds with coordinated water molecule, the CN of lutetium will be eight (Scheme 8).

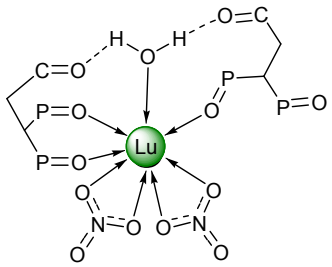

Scheme 8. Complex cation of compound **6** in $CDCl_3$ solution

This type of ligand coordination is not unique. A number of complexes are known where ligand forms H-bond with coordinated water molecule rather than coordination bond with metal.[35] The data of NMR spectroscopy agree well with the suggested structure (Scheme 8). Thus ^{31}P NMR spectrum shows a sole signal of phosphorus nuclei shifted by 9.1 ppm relative to free ligand signal ($W_{½}$ = 0.5 ppm) (Table 5). On cooling to – 50 °C, a second broadened resonance about 35 ppm, which may be related to uncoordinated P(O) group[36], appears along with the main broadened signal at ~ 40 ppm. Fast exchange processes with participation of coordinated and uncoordinated P(O) groups seem to take place in coordination sphere of Lu in complex **6** at ambient temperature. The ^{1}H and ^{13}C NMR spectra of complex **6** (Tables 6, 7) are as expected for the structure of complex cation in Scheme 8. Thus for ^{13}C the change on chemical shifts are $\Delta\delta_C(\underline{C}H_3)$ 0.17 ppm, $\Delta\delta_C(\underline{C}H_2)$ 1.11 ppm, $\Delta\delta_C(\underline{C}H)$ –3.68 ppm, and $\Delta\delta_C(C{=}O)$ 1.9 ppm. The signal of C=O group is broad. These changes are close to that observed for the spectrum of complex **3** and agree well with conclusion on the participation of C=O group in certain interactions. The changes in chemical shifts ($\Delta\delta_H$) for $C\underline{H}_3$ and $C\underline{H}_2$ groups also confirm the conclusion on the involvement of C=O group into "coordination". Water signal in the spectrum of **6** is at 5.4 ppm, whereas it is usually detected in chloroform at ~1.6 ppm.

It is possible that the this complex is in equilibrium with other complexes, for example, $[Lu\{P(O),P(O),C(O)\text{-}\mathbf{L}\}\{P(O),C(O)\text{-}\mathbf{L}\}(H_2O)(OO\text{-}NO_3)_2]^{+}\cdot(NO_3)^{-}$, where both C=O groups are weakly coordinated to the metal (CN = 10), neutral complex $[Lu\{P(O),P(O)\text{-}\mathbf{L}\}\{P(O)\text{-}\mathbf{L}\}(H_2O)(OO\text{-}NO_3)_3]$ (CN = 10), *etc*. However, CN = 10 is less typical for lutetium cation.

Thus, scorpionate ligand **L** in complexes with *f*-block element nitrates in chloroform show variable denticity. In the complex with uranyl nitrate **1**, this ligand is coordinated in P(O),P(O) bidentate mode like in the crystal. This kind of chelate coordination is not realized in chloroform solutions of complexes with lanthanide nitrates **3**–**6**. The main coordination is P(O),P(O)C(O)-tridentate, while P(O)C(O)-bidentate coordination, however through H-bond formation, is observed for the first time in lutetium complex.

It should be noted that almost all studied complexes are labile in solutions. Except for uranyl complex **1** in chloroform and AN, all other complexes have one or two broadened resonance in ^{31}P NMR spectra (Table 5). Although we did not conduct detailed study, we suppose that the structures shown in Schemes 4–8 and noted in the text are only the main species present in solutions. Virtually all studied complexes exhibit fluxional behavior in solutions.

Let us note that only monoligand uranyl complex $[UO_2(NO_3)_2\mathbf{L}]$ is neutral in chloroform solutions, all studied bisligand lanthanide complexes are cationic $[Ln(NO_3)_2(\mathbf{L})_2]^{+}\cdot(NO_3)^{-}$. This fact should be taken into account in analyzing the data on extraction of *f*-block elements from nitric acid solutions into chloroform.

Thus, the coordination mode of the scorpionate ligand **L** varies with not only requirements of metal coordination polyhedron and complex composition, but also depending on the solvent and shows large variety.

2.4. Extraction studies

The extraction ability of ligand **L** towards *f*-block elements was studied by the example of extraction of the group of lanthanides(III), as well as uranium(VI) from nitric acid solutions into $CHCl_3$. To compare the efficiency and selectivity of studied ligand **L** and well-known extractant **L'**, we compared the distribution ratios of *f*-block elements ($D = [M]_{org}/[M]_{aq}$) for both extractants under the same experimental conditions (Fig. 9, Table S2, ESI†).

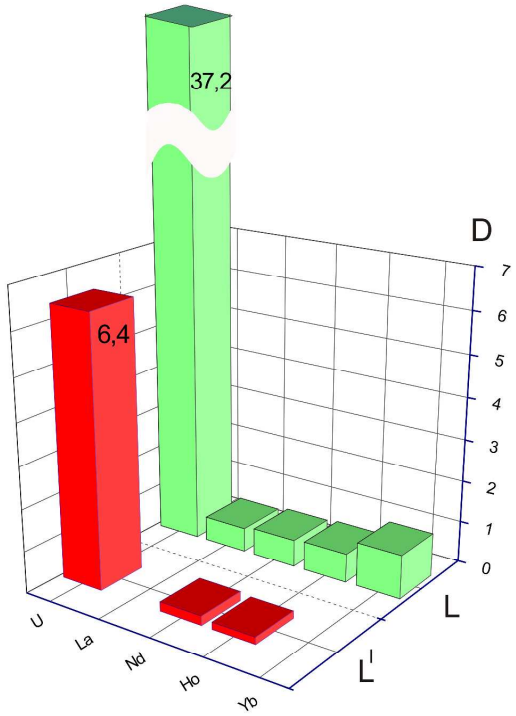

Fig. 9. Comparison of the distribution ratios of U(VI), La(III), Nd(III), Ho(III), and Yb(III) for the extraction with ligandes **L** and **L'** (0.01 M solutions in $CHCl_3$) from 3.75 M HNO_3; the initial concentration of lanthanide and uranyl nitrates in the aqueous phase is $2.5 \cdot 10^{-4}$ M.

Figure 9 shows that both compounds extract U(VI) much more efficiently than lanthanides. However, scorpionate ligand **L** extracts uranium by a factor of 6 more efficiently than its prototype **L'**. Fraction extracted for uranium over one step is 98%. Let us note that the values of D_U for common extractants – $(BuO)_3P(O)$, $(C_8H_{17})_3P(O)$, and $Ph_2P(O)CH_2C(O)NBu_2$ – is lower 1.0 under the same experimental conditions. Compound **L** also better (about 3 times) extracts lanthanides than ligand **L'**. Extraction selectivity U(VI)/Ln(III) of ligand **L** is higher than that of ligand **L'.**

As noted above, both ligands, **L** and **L'**, form with uranyl and lanthanide nitrates crystalline complexes of the same composition with the same chelate coordination of the phosphoryl groups. The π-stacking interaction between the Ph fragments of coordinated ligand molecules is inherent in not only ligand **L** but also to a lesser extent to ligand **L'** (Section 2.2.2). At the same time, the C=O group of scorpionate **L** in chloroform solutions of all lanthanide complexes participates in coordination along with two phosphoryl groups (Section 2.3.2). Judging from the spectral and X-

ray diffraction data, C=O→Ln bond in the studied complexes is rather weak; however, we believe that it is its formation that leads to better extraction of lanthanides with ligand **L**. It should be also noted that lanthanide complexes **3**–**6** in chloroform solutions are ionic in contrast to neutral uranyl complex **1**, which also favors better extraction of the latter. In uranyl complex **1**, the C=O group is not coordinated, however, it is available for other interactions. In crystal, the uncoordinated C=O group participate in various CH…O=C contacts and one can expect that its availability for interaction with diluent will favor better extraction of the corresponding compound.
Thus, the modification of methylene dioxide **L'** by the introduction of $MeC(O)CH_2$– substituent leads to considerable improvement of extraction properties of the hybrid scorpionate ligand **L** toward *f*-block elements.

3. Conclusion

Coordination properties of neutral organophosphorus scorpionate ligand **L** toward *f*-block elements were examined. Mono- and binuclear complexes of **L** with uranyl and lanthanide(III) nitrates were studied in solid state (X-ray, IR) and solutions (IR, ^{31}P NMR, ^{13}C NMR, and ^{1}H NMR). In the studied complexes, the ligand **L** exhibits variable denticity: PO,PO-, PO,PO,CO-. PO,CO-, and PO-. The C=O→Ln coordination bond is rather weak; at the same time, noncoordinated C=O group is involved into weak noncovalent interactions in both solution and crystal. Ligand coordination mode and complex structure are readily variable depending on both metal nature and interactions in the second coordination sphere. The extraction experiment revealed an expected increase in the affinity of scorpionate ligand **L** over its unmodified prototype **L'** for studied metal ions.

4. Experimental

General

Solvents were purified and dried using standard procedures. Deuterated solvents, CD_3CN (99.8% D, Sigma-Aldrich) and $CDCl_3$ (99.8% D, Sigma-Aldrich), were used as received. Multinuclear NMR spectra were recorded on a Bruker Avance 400 spectrometer, operating frequency 400.23 MHz (^{1}H and $^{1}H\{^{31}P\}$), 100.61 MHz (^{13}C) and 161.98 MHz (^{31}P and $^{31}P\{^{1}H\}$) at ambient temperature using CD_3CN or $CDCl_3$ solution (0.01 M), unless otherwise stated. Chemical shifts (ppm) are referred to the residual protic solvent peaks (for ^{1}H and ^{13}C), and 85 % H_3PO_4 (for ^{31}P) as external standards and coupling constants are expressed in hertz (Hz), the band width at half-height (W½) in ppm (for $^{31}P\{^{1}H\}$ NMR spectra). IR spectra in the region 400–4000 cm^{-1} were obtained on a Bruker Tensor 37 FTIR spectrometer. The samples were KBr pellets, mulls in Nujol and hexachlorobutadiene as well as 0.01 M solutions (CD_3CN, $CDCl_3$) in CaF_2 cuvettes, unless otherwise stated. Raman spectra of the solid samples were obtained in the region 100–3500 cm^{-1} using a Jobin–Yvon LabRAM 300 laser Raman spectrometer with 632.8 nm excitation of 2mW output power. Elemental analyses were performed at the Laboratory of Microanalysis, INEOS RAS.
The reagents *(E)*-4-(Diphenylphosphoryl)but-3-en-2-one[12] and methylenediphosphine dioxide (**L'**)[37] were prepared according to the literature procedures. Chlorodiphenylphosphine (Acros) was purified by vacuum distillation immediately prior to use. Glacial acetic acid (reagent grade) was distilled before reaction. Basic Brockmann activity grade I Al_2O_3, 50-200 μm (Acros) and silica gel 130-270 mesh, 60 Å (Aldrich) were used. Acetonitrile was dried by distillation over P_2O_5 prior to use. All manipulations with chlorodiphenylphosphine were carried out under an argon atmosphere.
The following reagents were used for the preparation of solutions in extraction study: bidistilled water, $CHCl_3$ (reagent grade), arsenazo III (analytical grade), HNO_3 (high purity grade), $UO_2(NO_3)_2 \cdot 6H_2O$ (reagent grade), $La(NO_3)_3 \cdot 6H_2O$ (reagent grade), $Nd(NO_3)_3 \cdot 6H_2O$ (reagent grade), $Ho(NO_3)_3 \cdot 6H_2O$ (pure grade), and $Yb(NO_3)_3 \cdot 6H_2O$ (pure grade). Solutions for spectral and extraction studies were prepared by volumetric/gravimetric method.

Synthesis of 4,4-bis(diphenylphosphoryl)butan-2-one (L). A solution of 0.250 g (3.85 mmol) of glacial acetic acid in 3 mL of anhydrous acetonitrile and next a solution of 0.793 g (3.6 mmol) of Ph_2PCl in 4 mL of anhydrous acetonitrile were added dropwise to a solution of 0.81 g (3 mmol) of (*E*)-4-(diphenylphosphoryl)but-3-en-2-one in 8 mL of anhydrous acetonitrile, the reaction mixture was kept for 48 h at ambient temperature, the solvent was removed in vacuum (~10 Torr) at ambient temperature, the oily residue was kept for 2 h at 55ºC at ~1 Torr, dissolved in 15 mL of CH_2Cl_2, the resultant solution was sequentially filtered through 3 g of basic alumina and 1.5 g of silica gel, with washing each sorbent with 15 ml of CH_2Cl_2, the filtrate was evaporated to dryness, the resultant foam-like residue was crystallized from benzene and dried in vacuum (~1 Torr) at 120 ºC until constant weight to give **L** (0.595 g, 42.1%). Mp 146.5-148.0 ºC (lit.[10] 145.0–145.5 ºC). Found: C, 71.23; H, 5.44; P, 13.13. Calc. For $C_{28}H_{26}O_3P_2$: C, 71.18; H, 5.55; P, 13.11 %. IR (KBr disk): ν_{max}/cm^{-1} 1720s (C=O), 1202s and 1182s (P=O). ^1H NMR (400 MHz, $CDCl_3$, 0.1 M): δ 1.54 (3H, s, CH_3,), 2.94 (2H, dt, $^3J_{HH}$ 5.3, $^3J_{HP}$ 14.5, CH_2), 4.45 (1H, tt, $^3J_{HH}$ 5.2, $^2J_{HP}$ 14.3, CH), 7.23–7.31 (8H, m, *m*–Ph), 7.31–7.38 (4H, m, *p*–Ph), 7.64–7.73 (4H, m, *o*–Ph), 7.76–7.85 (4H, m, *o*–Ph). $^1H\{^{31}P\}$ NMR (400 MHz, $CDCl_3$, 0.1 M): δ 1.55 (3H, s, CH_3), 2.94 (2H, d, $^3J_{HH}$ 5.0, CH_2), 4.46 (1H, t, $^3J_{HH}$ 5.1, CH), 7.23–7.31 (8H, m, *m*–Ph), 7.31–7.39 (4H, m, *p*–Ph), 7.68 (4H, d, $^3J_{HH}$ 7.7, *o*–Ph), 7.81 (4H, d, $^3J_{HH}$ 7.3, *o*–Ph). $^{13}C\{^1H\}$ NMR (100.61 MHz, $CDCl_3$, 0.1 M): δ 28.81 (s, CH_3), 36.73 (t, $^1J_{CP}$ 59.4, CH), 38.70 (s, CH_2), 128.10 (d, $^3J_{CP}$ 12.5, *m*–Ph), 128.12 (d, $^3J_{CP}$ 12.5, *m*–Ph), 130.82 (d, $^1J_{CP}$ 103.0, *ipso*–Ph), 131.33 (dd, $^1J_{CP}$ 100.6, $^3J_{CP}$ = 3.0, *ipso*–Ph), 131.45–131.53 (m, *p*–Ph), 131.48 (d, $^2J_{CP}$ 9.8, *o*–Ph), 131.52 (d, $^2J_{CP}$ 10.1, *o*–Ph), 131.63–131.71 (m, *p*–Ph), 203.84 (t, $^3J_{CP}$ 4.9, C=O). $^{31}P\{^1H\}$ NMR (161.98 MHz, $CDCl_3$, 0.1 M): δ 31.25 (s).

Synthesis of complexes 1, 3–6 (general). The complexes **1, 3–6**, including those suitable for X-ray analysis, were prepared according to a similar procedure, with the ratio of reagents of 1:1 or 1:2. The yields were 50–90%, but no attempts were made to optimize the yield for each individual complex.

$[UO_2(NO_3)_2L]$, **1**. a) A solution of $UO_2(NO_3)_2\cdot 6H_2O$ (106.2 mg, 0.212 mmol) in acetonitrile (1 mL) was added dropwise to a stirred solution of ligand L (100.0 mg, 0.212 mmol) in chloroform (1 mL) at room temperature. The resulting yellow precipitate was collected by filtration, washed with diethyl ether, and dried *in vacuo* (1 Torr) at 62 °C to give **1** (167.4 mg, 91%).
b) A solution of $UO_2(NO_3)_2\cdot 6H_2O$ (35.1 mg, 0.070 mmol) in acetonitrile (1.5 mL) was added dropwise to a stirred solution of ligand **L** (100.0 mg, 0.212 mmol) in chloroform (1 mL) at room temperature. The transparent light yellow solution was concentrated at ~ 60 °C in vacuo (~5 Torr) down to volume of ~ 1 mL. Light yellow transparent crystals of **1**, including suitable for X-ray diffraction studies, were obtained under cooling up to room temperature. The resulting yellow crystals were collected by filtration, washed with diethyl ether, and dried in air at r.t. to give **1** (30.0 mg, 50%). Mp 235-236 °C. Found: C, 38.56; H, 3.05; N, 3.01; P, 7.31; U, 27.89. Calc. for $C_{28}H_{26}N_2O_{11}P_2U$: C, 38.81; H, 3.02; N, 3.23; P, 7.15; U, 27.47%. IR (KBr disk): ν_{max}/cm^{-1} 1720s (C=O), 1166s (P=O), 1518s (N=O), 1308s and 1282s $(NO_2)_{as}$, 1032w $(NO_2)_s$, 939s $(O=U=O)_{as}$.
Raman: ν/cm^{-1} 858 $(O=U=O)_{as}$, 1037 $(NO_2)_s$. ^1H NMR (400.13 MHz, $CDCl_3$, ~ 0.003 M): δ 1.38 (3H, s, Me), 2.85 (2H, d.t., $^3J_{HH}$ 5.0, $^3J_{HP}$ 14.7, CH_2), 4.96 (1H, br m., CH), 7.18–7.22 (4H, m, *m*–Ph); 7.34–7.38 (2H, m, *p*–Ph); 7.63–7.68 (6H, m, *m*–+*p*–Ph); 7.84–7.89 (4H, m, *o*–Ph); 8.14–8.19 (4H, m, *o*–Ph). $^{13}C\{^1H\}$ NMR (100.61 MHz, $CDCl_3$, ~ 0.003 M): δ 28.84 (s, CH_3), 31.93 (s, CH), 37.72 (s, CH_2), 129.10–129.40 (m, Ph), 129.71–129.95 (m, Ph), 130.95–131.05 (m, Ph), 131.10–131.28 (m, Ph), 133.44 (s, Ph), 134.14 (s, Ph), 202.42s (s, C=O). No signals of *ipso*–Ph were observed. $^{31}P\{^1H\}$ (161.98 MHz, $CDCl_3$, ~ 0.003 M): δ 44.4 (s, W½ 0.03).

$[\{UO_2(NO_3)L\}_2(\mu_2\text{-}O_2)]\cdot EtOH$, **2**. Dissolution of precipitate of **1** in EtOH under heating led to the formation of a yellow clear solution. The solution was left to stand in ambient light for 4 week and produced by slow isothermal evaporation yellow solid and yellow crystalline material. Only a small number of crystals were yielded, and some of these proved for single crystal X-ray

diffraction. Elemental analysis and vibrational spectra could not be obtained because of the low yield of **2**.

[La(NO$_3$)$_3$L$_2$]·2.33 MeCN, **3**. A solution of La(NO$_3$)$_3$·6H$_2$O (40.2 mg, 0.09 mmol) in acetonitrile (2 mL) was added dropwise to a stirred solution of ligand **L** (87.7 mg, 0.18 mmol) in chloroform (0.5 mL) at room temperature. After addition of ten drops of anhydrous ether, a white precipitate formed, it was dissolved by addition of 1 mL of acetonitrile. After a while, a large amount of fine white needle-like crystals formed, some of them are suitable for X-ray diffraction study. The crystals were separated by decantation, washed with anhydrous ether and dried in air (108.5 mg, 81%). Mp (with decomp.) 153–159 °C. The elemental analysis indicated that the formula of crystals of **3** is La(NO$_3$)$_3$·(L)$_2$·2CH$_3$CN. Found: C, 53.20; H, 4.40; N, 5.01. Calc. for C$_{60}$H$_{58}$LaN$_5$O$_{15}$P$_4$: C, 53.30; H, 4.32; N, 5.18%. In the sample used for ^{1}H NMR spectrum, the presence only two acetonitrile molecules was found. The IR band and Raman lines of acetonitrile molecules were not observed in vibrational spectra of **3**. IR (KBr disk): ν_{max}/cm^{-1} 1716s (C=O), 1166s (P=O), 1458s (N=O), 1313s (NO$_2$)$_{as}$, 1031w (NO$_2$)$_s$. ^{1}H NMR (400.13 MHz, CDCl$_3$): δ 1.62 (3H, s, CH$_3$), 3.36 (2H, v br t, CH$_2$), 4.63 (1H, v br s, CH), 7.16–7.23 (4H, m, *m*–Ph), 7.24–7.30 (2H, m, *p*–Ph), 7.42–7.56 (6H, m, *m*+*p*–Ph), 7.82–8.00 (8H, br m, *o*–Ph), and 2.03 (6H, s, CH$_3$CN). ^{13}C{^{1}H} NMR (100.61 MHz, CDCl$_3$): δ 29.17 (s, CH$_3$), 32.4 (br s, CH), 39.2 (br s, CH$_2$), 128.65 (d, $^1J_{CP}$ 92.0, *ipso*–Ph), 128.86 (d, $^1J_{CP}$ 91.0, *ipso*–Ph), 128.70–129.70 (m, *m*-Ph), 131.12 (br s, *o*–Ph), 132.49 (s, *p*–Ph), 133.02 (s, *p*–Ph), 206.2 (br s, C=O), and 1.92 (s, *C*H$_3$CN), 116.4 (s, CH$_3$*C*N). ^{31}P{^{1}H} NMR (161.98 MHz, CDCl$_3$): δ 36.0 (br s, W$_{½}$ 0.7).

[Nd(NO$_3$)$_3$L$_2$]·3MeCN, 4. A solution of Nd(NO$_3$)$_3$·6H$_2$O (46.4 mg, 0.106 mmol) in acetonitrile (1 mL) was added dropwise to a stirred solution of ligand **L** (100 mg, 0.212 mmol) in chloroform (0.5 mL) at room temperature. The solution was concentrated at ~ 60 °C in vacuo (~5 Torr) down to volume of ~ 0.5 mL. Overnight light lilac fine-crystalline precipitate of **4** (94.5 mg, 70%) was filtered, washed by diethyl ether and dried in air. Mp (with decomp.) 147–150 °C. Found: C, 53.15; H, 4.30; N, 5.81. Calc. for C$_{62}$H$_{61}$N$_6$NdO$_{15}$P$_4$: C, 53.25; H, 4.40; N, 6.01%. On storage in air, especially upon trituration, the complex easily loses solvent of crystallization.[31] IR (KBr disk): ν_{max}/cm^{-1} 1717s (C=O), 1164s br (P=O), 1465(N=O), 1306s (NO$_2$)$_{as}$, 1030w (NO$_2$)$_s$. ^{1}H NMR (400.13 MHz, CD$_3$CN): δ 1.10 (3H, br s, CH$_3$), 4.1 (2H, v br s, CH$_2$), 7.04 (5H, br s, Ph), 7.31 (3H, br s, Ph), 7.67–7.83 (8H, br m, Ph), 8.82 (4H, v br s, Ph). No signal of CH was observed. ^{13}C{^{1}H} NMR (100.61 MHz, CD$_3$CN): δ 28.30 (s, CH$_3$), 29.9 (br s, CH), 39.3 (br s, CH$_2$), 128.90 (d, $^3J_{CP}$ 12.5, Ph), 129.79 (d, $^3J_{CP}$ 12.5, Ph), 131.62–131.90 (br m, Ph), 132.58 (br d, $^2J_{CP}$ 8.8, Ph), 133.01 (s, Ph), 133.66 (s, Ph), 205.4 (br s, C=O). No signals of *ipso*–Ph were observed.
^{31}P{^{1}H} (161.98 MHz, CD$_3$CN): δ 86 (br s, W$_{½}$ 2.5).

[Nd(NO$_3$)$_3$L$_2$] EtOH, 5. Complex **4** (40 mg) was dried in vacuo (~1 Torr) at 62 °C and dissolved in ~ 0.7 ml EtOH. After a few days light lilac fine-crystalline precipitate of **5** was filtered, washed by diethyl ether and dried in air (31 mg, 78%). Mp (with decomp.) 157–160 C. Found: C, 52.62; H, 4.34; N, 3.21. Calc. for C$_{58}$H$_{58}$N$_3$NdO$_{16}$P$_4$: C, 52.73; H, 4.42; N, 3.18%. IR (KBr disk): ν_{max}/cm^{-1} 1711 and 1722 sh (C=O), 1160s and 1150m (P=O), 1503, 1465(N=O), 1285, 1306 (NO$_2$)$_{as}$, 1030w (NO$_2$)$_s$, 1300–1500 wide absorption (NO$_3$, see Section 2.2.3), 3440 br (OH). NMR spectra of complex **5** are identical to those of complex **4** except for the signals of solvent of crystallization in ^{1}H and ^{13}C NMR spectra.

[Lu(NO$_3$)$_3$L$_2$], 6. A solution of Lu(NO$_3$)$_3$·3H$_2$O (43.9 mg, 0.106 mmol) in acetonitrile (1 mL) was added dropwise to a stirred solution of ligand **L** (100 mg, 0.212 mmol) in chloroform (1 mL) at room temperature. The solution was concentrated at ~ 60 °C in vacuo (~5 Torr) down to volume of ~ 0.5 mL. After addition of six drops of anhydrous ether, the solution became slightly turbid. Overnight white powder of **6** (94.5 mg, 70%) was filtered, washed by diethyl ether and dried in vacuo (~1 Torr) at 62 °C. Mp (with decomp.) 147–150 °C. Found: C, 51.33; H, 3.95; N, 3.26. Calc. for C$_{56}$H$_{52}$LuN$_3$O$_{15}$P$_4$: C, 51.51; H, 4.01; N, 3.22%. IR (KBr disk): ν_{max}/cm^{-1} 1721s (C=O),

1161s and 1185m (P=O), 1494s and 1518sh (N=O), 1310s $(NO_2)_{as}$, 1030w $(NO_2)_s$, 3200 br (OH). ^{1}H NMR (400.13 MHz, $CDCl_3$): δ 1.61 (3H, s, CH_3), 3.28 (2H, t, $^2J_{HP}$ 14.0, CH_2), 5.0 (1H, v br s, CH), 7.24–7.25 (4H, m, Ph), 7.34–7.41 (2H, t, Ph), 7.43–7.50 (4H, m, Ph), 7.52–7.59 (2H, m, Ph), 7.84–7.99 (8H, br m, Ph). ^{13}C{^{1}H} NMR (100.61 MHz, $CDCl_3$): δ 28.98 (s, CH_3), 33.05 (t, $^1J_{CP}$ 54.7, CH), 39.81 (s, CH_2), 127.51 (d, $^1J_{CP}$ 108.6, *ipso*–Ph), 127.85 (d, $^1J_{CP}$ 107.9, *ipso*–Ph), 128.80–129.15 (m, Ph), 129.20–129.15 (m, Ph), 131.00–131.42 (m, Ph), 133.09 (s, Ph), 133.42 (s, Ph), 205.7 (s, C=O). ^{31}P{^{1}H} NMR (161.98 MHz, $CDCl_3$): δ 40.3 (br s, $W_{½}$ 0.5).

Extraction of *f*-block elements

The distribution of U(VI), La(III), Nd(III), Ho(III), and Yb(III) in the extraction systems was studied in model solutions of 3.75 M nitric acid at the metal concentration 0.25 mM. Extractant solutions (0.01 M) in $CHCl_3$ were prepared from precisely weighed amounts of the reagents. The experiments were carried out in ampoules with ground stoppers at 20±1 °C. The volumes of both organic and aqueous phases were equal to 2 mL. The solution was stirred for 30 min at 80 rpm to achieve constant values of the distribution ratio ($D = [M]_{org}/[M]_{aq}$). After the extraction, 0.5mL of the aqueous solution was taken for further analysis. Metal concentrations in the initial and equilibrium aqueous solutions were determined by spectrophotometry.[38]

X-ray crystallography

The X-ray diffraction data were collected on a Bruker Apex II CCD diffractometer using Mo – Kα (λ = 0.71073 Å) radiation. The structures were solved by the direct method and refined by full-matrix least squares against F^2. Non-hydrogen atoms were refined in anisotropic approximation with an exception of disordered atoms. Oxygen atoms of uranyl cation in **2** are equally disordered over two sites and were refined isotropically. Occupation of solvate molecules in **2**–**5** was refined as a free variable giving full occupation with an exception of one MeCN solvent molecule in **3** which was further fixed at 1/3. Complex **3** crystallizes as twinned single crystal; twin components were separated using PLATON[39] and refined using HKLF 5 instruction and additional BASF factor. Hydrogen atoms were included in the refinement by the riding model with $U_{iso}(H) = nU_{eq}(C)$, where n = 1.5 for methyl and OH groups and 1.2 for the other atoms. All calculations were performed using SHELXL2013[40] and OLEX2.0[41] program packages.
CCDC 1442097-1442102 for compounds **L**, **1**–**5** contain the supplementary crystallographic data for this study.

Table 8. Crystallographic data and refinement parameters for **L**, **1**–**5**

Compound	**L** · $0.5C_6H_6$	**1**	**2**	**3**	**4**	**5**
Empirical formula	$C_{31}H_{29}O_3P_2$	$C_{28}H_{26}N_2O_{11}P_2U$	$C_{58}H_{58}N_2O_{19}P_4U_2$	$C_{60.67}H_{59}LaN_{5.33}O_{15}P_4$	$C_{62}H_{61}N_6NdO_{15}P_4$	$C_{58}H_{58}N_3NdO_{16}P_4$
Fw	511.48	866.48	1687.00	1365.59	1398.28	1321.19
Color, habit	Colorless, prism	Yellow, plate	Yellow, needle	Colorless, needle	Pink, needle	Pink, prism
Crystal size (mm^3)	0.23 × 0.18 × 0.15	0.23 × 0.18 × 0.10	0.29 × 0.08 × 0.08	0.29 × 0.08 × 0.08	0.31 × 0.08 × 0.06	0.23 × 0.19 × 0.11
F(000)	538	1672	3264	2789	2860	1350
T, K	148	100	100	120	120	120
Space group, *Z*	Triclinic, $P\bar{1}$, 2	Monoclinic, $P2_1/c$, 4	Orthorhombic, *Pbca*, 4	Monoclinic, *C2/c*, 4	Monoclinic, *C2/c*, 4	Triclinic, $P\bar{1}$, 2
a (Å)	9.8274(12)	11.3280(7)	18.2266(7)	13.444(8)	13.4706(8)	12.590(7)
b (Å)	11.8989(15)	13.8253(9)	17.8372(7)	17.849(9)	17.8919(10)	13.510(10)
c (Å)	13.0901(16)	19.7227(13)	19.0939(8)	26.571(15)	26.4711(15)	19.148(15)
α (°)	70.615(2)	90	90	90	90	90.574(16)
β (°)	68.839(2)	104.445(1)	90	90.709(14)	91.378(1)	96.836(16)
γ (°)	87.156(2)	90	90	90	90	111.923(17)
V ($Å^3$)	1342.3(3)	2991.2(3)	6207.6(4)	6375(6)	6378.1(6)	2994(4)
d_c (g/cm^3)	1.266	1.924	1.805	1.423	1.456	1.465
μ(MoKα) (cm^{-1})	0.193	5.597	5.387	0.839	0.984	1.043
θ_{max} (°)	29.00	31.77	27.00	25.96	31.62	29.906
I_{hkl} coll/uniq	16085 / 7124	34749 / 7917	62107 / 6743	11231 / 8846	44834 / 10755	38088 / 17037
R_{int}	0.042	0.055	0.052	-	0.027	0.145
Obs.refl. / *N* / restraints	5432 / 327 / 0	6105 / 398 / 0	4803 / 406 / 11	4827 / 394 / 14	10078 / 403 / 2	8453 / 752 / 41
R,[a] % [I > 2σ(I)]	0.047	0.028	0.065	0.099	0.023	0.078
R_w,[b] %	0.125	0.057	0.158	0.245	0.060	0.152
GOF[c]	1.02	1.04	1.06	1.03	1.06	1.03

[a] $R = \Sigma \| |F_o| - |F_c| | / \Sigma |F_o|$. [b] $R_w = [\Sigma(w(F_o^2 - F_c^2)^2)/\Sigma(w(F_o^2))]^{1/2}$. [c] GOF = $[\Sigma w(F_o^2 - F_c^2)^2/(N_{obs} - N_{param})]^{1/2}$

Computational details

Topological analysis of electron density according to Bader's ''Atoms in Molecules'' theory (AIM)[21] was performed in AIMAll[43] program. The electron density ρ(r) (ED) in wfx-format for AIM calculations was generated for complexes **1**–**5** in GAUSSIAN 09[44] software suite on DFT level of theory. The hybrid PBE0[45] functional and all-electron scalar relativistic basis set[46] for U and La atoms and 6-311+G** basis set[47] for other atoms were utilized. The geometry parameters were used like that obtained in X-ray experiment. Interaction energies estimated with Espinosa's correlation scheme $E_{cont} = -½V(r)$.[22] For paramagnetic ionic complex **5** simplified procedure was applied by reason of non-convergence SCF equation. π-Stacking energy evaluation was performed for "frozen" ligands in conformation that they adopt in complex **5**. This technique was checked in computation for complexes **1** and **4**. The difference in energies obtained by simplified and complete procedures is not larger than 0.02 kcal/mol.

Acknowledgement

This work was supported by the Russian Foundation for Basic Research (Grant No. 14-03-00695)

Notes and references

1. For reviews, see (a) A. E. V. Gorden, M. A. DeVore, B. A. Maynard, *Inorg. Chem.,* 2013, **52**, 3445; (b) E. V. Sharova, O. I. Artyushin, I. L. Odinets, *Russ. Chem. Rev*., 2014, **83,** 95; (c) D. Rosario-Amorin, S. Ouizem, D. A. Dickie, Y. Wen, R. T. Paine, J. Gao, J. K. Grey, A. de Bettencourt-Dias, B. P. Hay, L. H. Delmau, *Inorg. Chem.,* 2013, **52**, 3063; (d) P. Tkac, G. F. Vandegrift, G. J. Lumetta, A. V. Gelis, *Ind. Eng. Chem. Res.*, **2012**, **51**, 10433; (e) S. Tachimori, Y. Morita, in *Ion exchange and solvent extraction*, ed. B.A. Moyer, CRC Press, 2010, v.**19**, pp. 1-64; (f) V. Manchanda, P.N. Pathak, P.K. Mohapatra, in *Ion exchange and solvent extraction*, ed. B.A. Moyer, CRC Press, 2010, v.**19**, pp. 66-118; (g) C. Hill, in *Ion exchange and solvent extraction*, ed. B.A. Moyer, CRC Press, 2010, v.**19**, pp. 119-194; (h) V. A. Babain, in *Ion exchange and solvent extraction*, ed. B.A. Moyer, CRC Press, 2010, v.**19**, pp. 359-380.
2. A. M. Rozen, B. V. Krupnov, *Russ. Chem. Rev.*, 1996, **65**, 973;
3. H. J. Cristau, D. Virieux, J. F. Dozol, H. Rouquette, *J. Radioanalyt. Nucl. Chem.,* 1999, **241**, 543;
4. I. V. Smirnov, *Radiokhimiya (in Russian)*, 2007, **49**, 44;
5. (a) A. N. Turanov, V. K. Karandashev, and N. A. Bondarenko, *Radiokhimiya (in Russian)*, 2007, **49**, 55; (b) A. N. Turanov, V. K. Karandashev, A. N. Yarkevich, and Z. V. Safronova, *Solv. Extr. Ion Exch*., 2004, **22**, 391; (c) T. Yaita, S. Tachimori, *Radiochim. Acta,* 1996, **73**, 27; (d) A.N. Turanov, V.K. Karandashev, V.E. Baulin, A.N. Yarkevich, S.V. Nosenko, *Radiokhimiya (in Russian),* 2012, **54**, 363; (e) A.N. Turanov, V.K. Karandashev, A.N. Yarkevich, Z.V. Safronova, *Radiokhimiya (in Russian),* 2011, **53**, 264; (f) N. E. Kochetkova, O. E. Kojro, N. P. Nesterova, T. Ya. Medved', M. K. Chmutova, B. F. Myasoedov, M. I. Kabachnik, *Radiokhimiya (in Russian)*, 1986, **28**, 338; (g) A. Yu. Shadrin, I. V. Smirnov, R. N. Kiseleva, N. P. Nesterova, Yu. M. Polikarpov, M. I. Kabachnik, *Radiokhimiya (in Russian)*, 1993, **35**, 50.
6. A. M. J. Lees, A. W. G. Platt, *Inorg. Chem.*, 2003, **42**, 4673.
7. S. Kannan, N. Rajalakshmi, K. V. Chetty, V. Venugopal, M. G. B. Drew, *Polyhedron* 2004, **23**, 1527.
8. (a) S. M. Cornet, I. May, M. P. Redmond, A. J. Selvage, C. A. Sharrad, O. Rosnel, *Polyhedron,* 2009, **28**,363; (b) N. J Hill, W. Levason, M. C Popham, G. Reid, M. Webster, *Polyhedron,* 2002, **21**, 445; (c) A. D. Sutton, G. H. John, M. J. Sarsfield, J. C. Renshaw, I. May, L. R. Martin, A. J. Selvage, D. Collison, M. Helliwell, *Inorg. Chem*., 2004, **43**, 5480.
9. P. E. Sues, A. J. Lough, R. H. Morris, *Inorg. Chem*., 2012, **51**, 9322.

10. A. N. Turanov, V. K. Karandashev, G. V. Bodrin, E. I. Goryunov, V. K. Brel, *Radiokhimiya (in Russian),* 2015, **57**, 509.
11. J. B. Conant, J. B. S. Braverman, R. E. Hussey, *J. Am. Chem. Soc.,* 1923, **45**, 165.
12. E. I. Goryunov, G. V. Bodrin, I. B. Goryunova, Yu. V. Nelyubina, P. V. Petrovskii, T. V. Strelkova, A. S. Peregudov, A. G. Matveeva, M. P. Passechnik, S. V. Matveev, E. E. Nifantrev, *Russ. Chem. Bull., Int. Ed.*, 2013, **62**, 780.
13. Geometry optimization and normal coordinate analysis for the X-ray conformation of **L** were carried out using DFT at PBE level by Priroda 6 program package (2006.08.20) [D.N. Laikov, *Chem. Phys. Lett.*, 1997, **281**, 151; D.N. Laikov, Yu. A. Ustynyuk, *Russ. Chem. Bull., Int. Ed.*, 2005, **54**, 820; J. P, Perdew, K. Bruke, M. Ernzerhof, *Phys. Rev. Lett.*, 1996, **77**, 3865].
14. (a) G. A. Doyle, D. M. L. Goodgame, A. Sinden, D. J. Williams, *Chem. Commun.,* 1993, 1170; (b) G. H. John, I. May, M. J. Sarsfield, H. M. Steele, D. Collison, M. Helliwell, J. D. McKinney, *Dalton Trans.*, 2004, 734; (c) B. T. McGrail, L. S. Pianowski, P. C.Burns, *J. Am. Chem. Soc.*, 2014, **136**, 4797.
15. W. D. Wang, A. Bakas, J. H. Espenson, *Inorg. Chem.*, 1995, **34**, 6034.
16. S. Wahu, J.-C. Berthet, P. Thuéry D. Guillaumont, M. Ephritikhine, R. Guillot, G. Cote, C. Bresson, *Eur. J. Inorg. Chem.,* 2012, 3747.
17. I. A.Charushnikova, C. Den Auwer, *Russ. J. Coord.Chem*. 2004, **30**, 546.
18. N. Akbarzadeh-T, T. Kondori, *Res.Chem.Intermed.,* 2015, **41**, 845.
19. See for example (a) P. Charpin, G. Folcher, M. Lance, M. Nierlich, D. Vigner, *Acta Crystallogr., C,* 1985, **41**, 1302; (b) B. Masci, P. Thuery, *Polyhedron,* 2005, **24**, 229; (c) G. A. Doyle, D. M. L. Goodgame, A. Sinden, D. J. Williams, *Chem. Commun.*, 1993, 1170; (d) I. M. Aladzheva, O. V. Bykhovskaya, Y. V. Nelyubina, Z. S. Klemenkova, P. V. Petrovskii, I. L. Odinets, *Inorg.Chim.Acta*, 2011, **373**, 130.
20. L. Huang, B.-Q. Ma, C.-H. Huang, T. C. W. Mak, G.-Q. Yao, G.-X. Xu, *J. Coord. Chem.,* 2001, **54**, 95.
21. R. F. W Bader, *Atoms in Molecules. A Quantum Theory*, Clarendron Press, Oxford, 1990.
22. (a) E. Espinosa, E. Molins, C. Lecomte, *Chem. Phys. Lett.,* 1998, **285,** 170; (b) E. Espinosa, I. Alkorta, I. Rozas, J. Elguero, E. Molins, *Chem. Phys. Lett.,* 2001, **336**, 457.
23. For example (a) A. A. Korlyukov, M. Yu Antipin, *Russ. Chem. Rev*., 2012, **81**, 105; (b) A. A. Korlyukov, *Russ. Chem. Rev*., 2015, **84**, 422; (c) C. Matta, R. J. Boyd, *The Quantum Theory of Atoms in Molecules*, Wiley-VCH, Weinheim, Germany, 2007; (d) I. V. Glukhov, K. A. Lyssenko, A. A. Korlyukov, M. Yu. Antipin, *Faraday Discuss.*, 2007, **135**, 203;
24. J. Overgaard, M. P. Waller, R. Piltz, J. A. Platts, P. Emseis, P. Leverett, P. A. Williams, D. E. Hibbs, *J. Phys. Chem. A*, 2007, **111**, 10123.
25. A. G. Matveeva, Z. A. Starikova, R. R. Aysin, R. S. Skazov, S. V. Matveev, G. I. Timofeeva, M. P. Passechnik, E. E. Nifant'ev, *Polyhedron,* 2013, **61,** 172.
26. R. K. Castellano, F. Diederch, E. A. Mayer, *Angew. Chem., Int. Ed.,* 2003, **42**, 1210.
27. See for example (a) M. B. Jones, A. J. Gaunt, *Chem. Rev.*, 2013, **113**, 1137; (b) B. G. Vats, S. Kannan, K. Parvathi, D. K. Maity, M. G. B. Drew, *Polyhedron,* 2015, **89**, 116; A. G. Matveeva, M. S. Grigoriev, T. K. Dvoryanchikova, S. V. Matveev, A. M. Safiulina, O. A. Sinegribova, M. P. Passechnik, I. A. Godovikov, D. A. Tatarinov, V. F. Mironov, I. G. Tananaev, *Russ. Chem. Bull., Int. Ed.*, 2012, **61**, 399.
28. (a) A. G. Matveeva, A. S. Peregudov, E. I. Matrosov, Z.A. Starikova, S. V. Matveev, E. E. Nifant'ev, *Inorg. Chim. Acta.,* 2009, **362**, 3607; (b) W. Levason, E. H Newman, M. Webster, *Polyhedron*, 2000, **19**, 2697; (c) M. Bosson, W. Levason, T. Patel, M. C. Popham, M. Webster, *Polyhedron*, 2001, **20**, 2055; (d) A. Bowden, S. J. Coles, M. B. Pitak, A. W. G. Platt, *Polyhedron,* 2014, **68**, 258; (e) A. Bowden, P. N. Horton, A. W. G. Platt, *Inorg. Chem*., 2011, **50**, 2553; (f) N.J. Hill, W. Levason, M.C. Popham, G. Reid, M. Webster, *Polyhedron*, 2002, **21,** 445.
29. See for example (a) R. Babecki, A. W. G. Platt, J. Fawcett, *J. Chem. Soc. Dalton Trans*., 1992, 675; (b) B.G. Vats, S. Kannan, I. C. Pius, D. M. Noronha, D. K. Maity, M. G. B. Drew, *Polyhedron*, 2014, **75**, 81.

30. CH…O=C contacts were revealed in the ligand **L** (r(H...O) = 2.4/2.6-2.8 Å for intra- and intermolecular interactions) and uranyl complex **1** (r(H...O) = 2.3–3.0/2.6–2.7 Å), however, they are much weaker than in complexes **3** and **4** (Fig. S1–S3, ESI). Accordingly, the IR spectra of **L** and complex **1** display ν(C=O) at 1720 cm^{-1}.
31. K. Nakamoto, *IR and Raman Spectra of Inorganic and Coordination Compounds*, Wiley, New York, 5th edn, 1997, Part B, 432 pp.
32. Vibrations of the C≡N group have low intensity. Moreover, solvate acetonitrile molecules are poorly retained in the crystal lattice of the studied complexes. Thus, freshly prepared finely crystalline complex **4** when stored in air becomes amorphous in time according to X-ray powder diffraction. The content of MeCN in **3**, **4** according to elemental analysis data and NMR is lower than that determined by X-ray crystallography.
33. For example, CN of ytterbium, whose radius is close to that of lutetium, equals to eight in the crystalline complex of akin ligand $[Yb(NO_3)(\mathbf{L'})_3](NO_3)_2 \cdot 2H_2O$.[6]
34. (a) A. Bowden, K. Singh, A. W. G. Platt, *Polyhedron*, 2012, **42**, 30; (b) A. G. Matveeva, T. V. Baulina, Z. A. Starikova, M. S. Grigor'ev, Z. S. Klemenkova, S. V. Matveev, L. A. Leites, R. R. Aysin, E. E. Nifant'ev, *Inorg. Chim. Acta*, 2012, **384**, 266.
35. (a) D. Das, S. Kannan, D. K. Maity, M. G. B. Drew, *Inorg. Chem*. 2012, **51**, 4869; (b) C. Villiers, P. Thuéry, M. Ephritikhine, *Polyhedron,* 2004, **23**, 1613; (c) D. J. McCabe, E. N. Duesler, R. T. Paine, *Inorg. Chem.,* 1985, **24**, 4626; (d) S. M. Bowen, E. N.Duesler, R. T. Paine, *Inorg. Chim. Acta,* 1982, **61**, 155;
36. In the spectra of lanthanide nitrate complexes with polydentate bisphosphoryl-containing ligands, the signal of uncoordinated P(O) group is usually broadened and slightly shifted downfield relative to free ligand signal.[28a,34b]
37. E. N. Tsvetkov, N. A. Bondarenko, I. G. Malakhova, M. I. Kabachnik, *Zh. Obshch. Khim. (in Russian)*, 1985, **55**, 11.
38. S. B. Savin, *Arsenazo III*, Atomizdat, Moscow, 1966, 256 pp. (in Russian).
39. A. L. Spek, *Acta Cryst.*, 2009, **D65**, 148.
40. G. M. Sheldrick, *Acta Cryst.*, 2008, **A64**, 112.
41. O. V. Dolomanov, L. J. Bourhis, R. J. Gildea, J. A. K. Howard, H. Puschmann, *J. Appl. Cryst.* 2009, **42**, 339.
42. AIMAll (Version 10.05.04), Todd A. Keith, TK Gristmill Software, Overland Park KS, USA, 2012 <aim.tkgristmill.com>
43. Gaussian 09, Revision D.01, M. J. Frisch, G. W. Trucks, H. B. Schlegel, G. E. Scuseria, M. A. Robb, J. R. Cheeseman, G. Scalmani, V. Barone, B. Mennucci, G. A. Petersson, H. Nakatsuji, M. Caricato, X. Li, H. P. Hratchian, A. F. Izmaylov, J. Bloino, G. Zheng, J. L. Sonnenberg, M. Hada, M. Ehara, K. Toyota, R. Fukuda, J. Hasegawa, M. Ishida, T. Nakajima, Y. Honda, O. Kitao, H. Nakai, T. Vreven, J. A. Montgomery, Jr., J. E. Peralta, F. Ogliaro, M. Bearpark, J. J. Heyd, E. Brothers, K. N. Kudin, V. N. Staroverov, T. Keith, R. Kobayashi, J. Normand, K. Raghavachari, A. Rendell, J. C. Burant, S. S. Iyengar, J. Tomasi, M. Cossi, N. Rega, J. M. Millam, M. Klene, J. E. Knox, J. B. Cross, V. Bakken, C. Adamo, J. Jaramillo, R. Gomperts, R. E. Stratmann, O. Yazyev, A. J. Austin, R. Cammi, C. Pomelli, J. W. Ochterski, R. L. Martin, K. Morokuma, V. G. Zakrzewski, G. A. Voth, P. Salvador, J. J. Dannenberg, S. Dapprich, A. D. Daniels, O. Farkas, J. B. Foresman, J. V. Ortiz, J. Cioslowski, and D. J. Fox, *Gaussian,* Inc., Wallingford CT, 2013.
44. J. P. Perdew, K. Burke, M. Ernzerhof, *Phys. Rev. Lett.*, 1997, **78**, 1396.
45. (a) D. A. Pantazis, F. Neese, *J. Chem. Theory Comput*., 2009, **5**, 2229; (b) D. A. Pantazis, F. Neese, *J. Chem. Theory Comput*., 2011, **7**, 677.
46. (a) R. Krishnan, J. S. Binkley, R. Seeger, J. A. Pople, *J. Chem. Phys*., 1980, **72,** 650;(b) A. D. McLean, G. S. Chandler, J. *Chem. Phys.* 1980, **72**, 5639.

Extraction and coordination studies of carbonyl−phosphine oxide scorpionate ligand with uranyl and lanthanide(III) nitrates: structural, spectroscopic and DFT characterization of complexes in solid state and solutions

Anna G. Matveeva, Anna V. Vologzhanina, Evgenii I. Goryunov, Rinat R. Aysin, Margarita P. Pasechnik, Sergey V. Matveev, Ivan A. Godovikov, Alfiya M. Safiulina, Valery K. Brel*

A graphical and textual abstract for the Table of contents entry.

Scorpionate organophosphorus ligand exhibits promising extraction properties and variable denticity in *f*-block element complexes in solid state and solutions.